COVID-19 Test Allocation Strategy to Mitigate SARS-CoV-2 Infections across School Districts

Remy Pasco, Kaitlyn Johnson, Spencer J. Fox, Kelly A. Pierce, Maureen Johnson-León, Michael Lachmann, David P. Morton, Lauren Ancel Meyers

In response to COVID-19, schools across the United States closed in early 2020; many did not fully reopen until late 2021. Although regular testing of asymptomatic students, teachers, and staff can reduce transmission risks, few school systems consistently used proactive testing to safeguard return to classrooms. Socioeconomically diverse public school districts might vary testing levels across campuses to ensure fair, effective use of limited resources. We describe a test allocation approach to reduce overall infections and disparities across school districts. Using a model of SARS-CoV-2 transmission in schools fit to data from a large metropolitan school district in Texas, we reduced incidence between the highest and lowest risk schools from a 5.6-fold difference under proportional test allocation to 1.8-fold difference under our optimized test allocation. This approach provides a roadmap to help school districts deploy proactive testing and mitigate risks of future SARS-CoV-2 variants and other pathogen threats.

By early January 2023, the COVID-19 pandemic had caused >6.7 million deaths worldwide (*1*), and severe socioeconomic hardship (*2*–*4*), particularly for racial minorities (*5*,*6*). Children experienced pandemic-related school closures that led to substantial losses in learning (*7*–*9*), elevated rates of child abuse (*10*), lack of access to healthy food (*11*), and emotional harm (*12*). By the end of March 2020, all kindergarten through 12th grade (K–12) public schools in the United States had stopped in-person instruction (*13*), affecting 55 million students. Schools in 48 US states remained closed through the end of the school year (*14*). In August and September of 2020, a total of 74% of the 100 largest school districts in the United States started the year with remote-only teaching (*15*). By November 2020, 19% of those districts remained fully remote, and 36% had fully resumed in-person learning (*15*). Schools continued to reopen throughout the year.

By September 2021, a large fraction (70%) of US adults had been vaccinated with highly effective SARS-CoV-2 vaccines (*16*), including an estimated 86% of K–12 teachers and school staff (*17*). However, children <12 years of age were still ineligible for vaccines (*16*,*18*). Because large pockets of the country were still unvaccinated, COVID-19 continued to claim lives, and 100,000 deaths were reported in the United States during July–September 2021, including 246 deaths among children 0–17 years of age (*16*). At the end of October 2021, the United States authorized administration of COVID-19 vaccines for children 5–11 years of age (*19*). In January 2022, schools returned from winter break amidst a major COVID-19 wave fueled by the emergence of the highly transmissible and immune-evasive Omicron variant (F.P. Lyngse, unpub. data, https://doi.org/10.1101/2021.12.27.21268278), and case counts among students and staff reached record numbers despite increasing vaccine coverage in the United States (*16*,*20*).

Schools across the country adopted diverse reopening plans for the 2021–22 school year. Among the largest districts, 96% offered some form of in-person learning (*21*). Although some schools fully returned to prepandemic normal operations without COVID-19 interventions, many adopted policies for using masks, social distancing, quarantine, or testing requirements to safeguard the return to campus. The federal government invested $122 billion to support safe, in-person instruction through screening, improved building ventilation, purchase of personal protective equipment, hiring of additional personnel,

Author affiliations: The University of Texas at Austin, Austin, Texas, USA (R. Pasco, K. Johnson, S.J. Fox, K.A. Pierce, M. Johnson-León, L.A. Meyers); Santa Fe Institute, Santa Fe, New Mexico, USA (M. Lachmann, L.A. Meyers); Northwestern University, Evanston, Illinois, USA (D.P. Morton)

DOI: https://doi.org/10.3201/eid2903.220761

and other measures (*22*,*23*). Within the first 2 months of the school year, ≈1.5% of schools closed temporarily in response to COVID-19 outbreaks (*21*).

Frequent and systematic testing of asymptomatic persons has been shown to be a viable and cost-effective mitigation strategy in communities, universities, and schools (*24*–*29*). However, tests are costly and inaccessible for many school districts in the United States; districts with limited testing resources are forced to determine how to allocate testing across schools to protect their students, staff, and communities. Some districts have opted to restrict testing to symptomatic persons and other districts have apportioned tests according to school enrollment (*30*,*31*).

In this study, we propose a strategy for allocating testing resources across a diverse school district in which the frequency of testing depends on the school's enrollment and grade range, recent COVID-19 cases reported among students and staff, and the estimated prevalence in the surrounding (i.e., catchment) community. Coupling derivative-free constrained optimization and a detailed agent-based simulation of SARS-CoV-2 transmission within and between classrooms, we derived an optimal allocation of tests across a school system that could minimize the maximum risk for cumulative infections on any campus over a 10-week period. We applied our approach to design a testing strategy for the 11 main high schools in the Austin Independent School District (AISD; Austin, Texas, USA), which has 18,500 enrolled students and 1,500 staff (*32*).

Methods

To determine an optimal allocation of tests across schools we developed a 2-step framework in which we first modeled COVID-19 transmission within schools for different levels of surveillance testing and then used those results as an input to an optimization model (Appendix, https://wwwnc.cdc.gov/EID/article/29/3/22-0761-App1.pdf). We first considered a hypothetical school system with 6 schools of 500 students each that differ over 2 parameters: community incidence and in-school transmission rate. For community incidence, we considered low and high scenarios. In the low scenario, the community had 35 new daily cases/100,000 persons; in the high scenario the community had 70 new daily cases/100,000 persons. For the transmission rate, we considered unmitigated R_0 values to be low (1.0), moderate (1.5), or high (2.0).

We then modeled 11 high schools in AISD by using student enrollment based on attendance in early January 2021. We considered 2 different in-school transmission rate scenarios: an unmitigated transmission rate in all schools of with an R_0 of 1.0; and transmission rates of each school estimated by fitting a regression model of the number of cases reported in that school against the estimated enrollment (*33*) (Appendix).

For each school and each scenario, we ran 300 stochastic simulations. We assumed that only students (not adult staff) were tested on Monday mornings and that test results were available instantly (*34*); preliminary analysis suggested that testing adults had minimal effects. During any given week, students in the model were selected for testing evenly across classes rather than testing a subset of entire classes.

In addition to proactive testing, we assumed that 90% of symptomatic persons would seek testing 0.5–1.5 days after symptom onset and then isolate after testing, even before results are available. We assumed 20% of infected students and 57% of infected adults would become symptomatic (*35*,*36*).

In our analysis of a hypothetical school system, we assumed that tests were perfectly accurate and that a positive test immediately triggered a 14-day isolation of the person and a 14-day quarantine of household and classroom members. For our case study of AISD, we assumed lower test accuracy based on estimates for the widely used Abbott BinaxNow antigen tests (https://www.abbott.com), which had 95% sensitivity for symptomatic persons, 80% sensitivity for asymptomatic persons, and 99% specificity (*37*,*38*).

Transmission Model

We built a stochastic agent-based model of COVID-19 transmission within schools that included household transmission for students. We held the average community incidence constant through the simulation and all persons could become infected through outside interactions that were not explicitly modeled. The modeled population included students, teachers, staff, bus drivers, and members of the students' households. We modeled various contacts between agents in schools (Appendix).

We used published estimates for the average SARS-CoV-2 incubation, latent, and infectious periods, as well as a person's infectiousness through time (*39*). We assumed that asymptomatic cases were two thirds as infectious as symptomatic cases (*40*).

We simulated contacts at half-hour intervals and stochastically determined infection events based on the transmission probability between pairs of interacting persons. For each scenario, we derived the transmission rate to produce the specified unmitigated in-school R_0 (Appendix). This R_0 is the basic

reproductive rate we would obtain without any testing, symptomatic or surveillance, and reflects other mitigation measures in place, such as face masks or social distancing.

We ran simulations for 10 weeks. We initiated simulations with everyone susceptible and simulated community and household infections for 10 days before school started.

Optimization Model

The objective of our test-allocation problem was to minimize the maximum risk experienced by any school in the system under consideration. Because of the stochastic nature of our COVID-19 transmission model, we had to choose a measure that summarized the risk for a given school under each possible frequency of surveillance testing. We defined the risk for each school as the expected number of on-campus infections of students plus the 90% conditional value-at-risk (CVaR) of the number of on-campus infections. Here, CVaR represents the expected number of such infections, conditional on restricting attention to the worst 10% of simulated outcomes, and hence accounts for risk aversion. Given 2 candidate allocations with a similar average number of cases, we preferred the allocation that limited the upside tail risk in terms of a large outbreak. We further accounted for risk by taking the worst-case risk measure across all schools. We used on-campus infections, rather than total infections, because total infections are partially driven by community incidence rather than school interventions. We further used the proportion of a school's infected population rather than the absolute number of infections, which enabled us to treat large and small schools equally. Then, we could calculate each school's risk as a function of the number of tests allocated; more tests reduced the risk incurred. Our goal was to allocate tests to schools to minimize the largest risk measure incurred at any school, subject to the constraints that we respect total testing capacity across the school system and that we cannot test all students at a school more than once per week (Appendix Figure 13).

Results

Under all transmission scenarios, we expected proactive testing to greatly reduce the proportion of students infected on campus over a 10-week period (Figure 1, panel A). In the high-risk scenario (in-school R_0 = 2.0), 14-day testing reduced the fraction of students infected from 18.2% to 4.1%; under the lowest risk scenario (in-school R_0 = 1.0), the expected incidence decreased from 4.0% to 1.5%. When we increased testing frequency from every 14 days to every 7 days, the expected incidence in high-risk scenario reduced to 2.1% and expected incidence in low-risk scenario reduced to 1.0%.

The efficacy of testing to mitigate in-school transmission depended on whether quarantine was limited

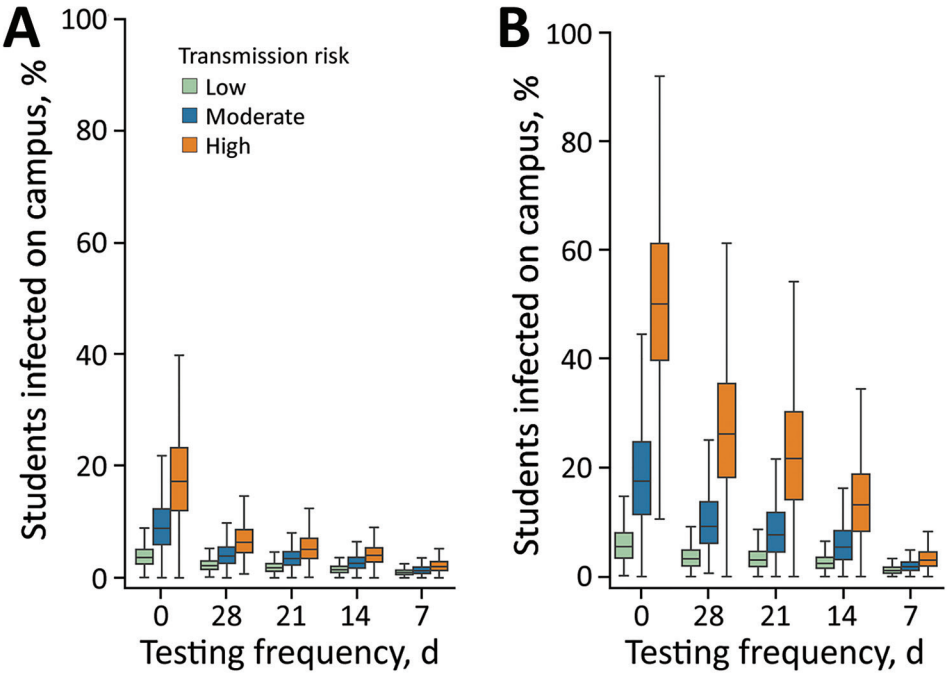

Figure 1. Projected effects of a COVID-19 test allocation strategy to mitigate SARS-CoV-2 infections across 11 school districts in the Austin Independent School District, Austin, Texas, USA. The whisker plots demonstrate projected effects over a 10-week period in a school with 500 students under 2 scenarios: A) assuming the household and classroom of each detected case is quarantined; or B) assuming only households (not entire classrooms) are quarantined. Colors indicate reproduction numbers as low (1.0), moderate (1.5), and high (2.0) in-school transmission risks in the absence of proactive or symptomatic testing, isolation, and quarantine. Whiskers indicate points that lie within 1.5 interquartile ranges of the lower and upper quartiles; boxes indicate interquartile range and horizontal bars indicate median fraction of students infected on-campus depending on the frequency of proactive testing as never (0), or once per every 28, 21, 14, or 7 days. Results are based on 300 stochastic simulations for each scenario.

to the household of the positive case or extended to the entire classroom (Figure 1, panel B). Under a moderate transmission scenario (in-school R_0 = 1.5) in which students are tested every other week, the expected incidence decreased from 6.3% (95% CI 1.0%–15.6%) to 2.9% (95% CI 1.0%–6.2%) when we added classroom quarantine to household quarantine. We also estimated the costs of quarantine in terms of days of in-school education lost over the 10-week projection period, under the moderate transmission risk scenario (Figure 2, panel A; Appendix 11). Without proactive testing, we expected the strategy of quarantining entire classrooms after a positive test to result in an average of 3 (6%) out of 50 school days missed per student. We expected household-only quarantine to reduce that cost by roughly 6.5-fold, to an average 0.9% of school days missed; however, that strategy roughly doubled the days students spent at school while infectious (Figure 2, panel B).

Regardless of quarantine policy, our model showed that proactive testing could reduce in-school exposure, with few to no additional lost days of school. In addition, we found that shortening the quarantine period for classroom contacts from 14 to 7 days would mitigate some of the educational losses without substantially increasing health risks (Appendix Figure 12).

As a sensitivity analysis, we also considered a higher rate of SARS-CoV-2 introductions from the surrounding community by raising daily new cases from 35 cases/100,000 persons to 70 cases/100,000 persons and lowering the accuracy of SARS-CoV-2 tests (*37*,*38*) (Appendix Figures 10, 11). In our sensitivity analysis, we found that our estimates were robust to the assumed sensitivity and specificity of the tests (Appendix).

Case Study—Optimizing Testing across a Large Municipal School District

We applied our model to derive an optimal allocation of testing resources across the 11 high schools in AISD, the largest district in Austin, Texas, which includes 75,000 students, 5,500 teachers, and 5,000 staff. The district operates 125 schools from pre-K–12th grade; 55% of students are Hispanic and 30% White, and >50% come from economically disadvantaged backgrounds (*32*). We estimated the external force of infection for each school by comparing reported COVID-19 incidence in the neighborhood of a school to reported incidence across the entire metropolitan statistical area (MSA) from March 2020–January 2021 (Figure 3, panel A) (*41*). We listed the schools in order of the estimated external risks; the catchment of school A had almost double (195%) the city-wide incidence, and the catchment of school K had only 37%. In general, risk (i.e., COVID-19 incidence) was higher on the east side of Austin.

We estimated on-campus transmission risk for each school by using reported cases from each school during August 16, 2020–March 8, 2021 (Figure 3, panel B). In brief, we scaled the in-school R_0 based on the difference between the cumulative, per student incidence in a school to the cumulative incidence throughout the district. We assumed a baseline R_0 of 1.0; thus, schools with incidence equal to the district-wide incidence had resulting estimates that ranged from 0.70–1.41. Our estimates for on-campus transmission risk and external force of infection were not greatly correlated (Appendix). We also ran scenarios in which all schools had the same transmission risk (Appendix Figures 5, 6).

On the basis of the estimated heterogeneity in risks across the district, we estimated the optimal

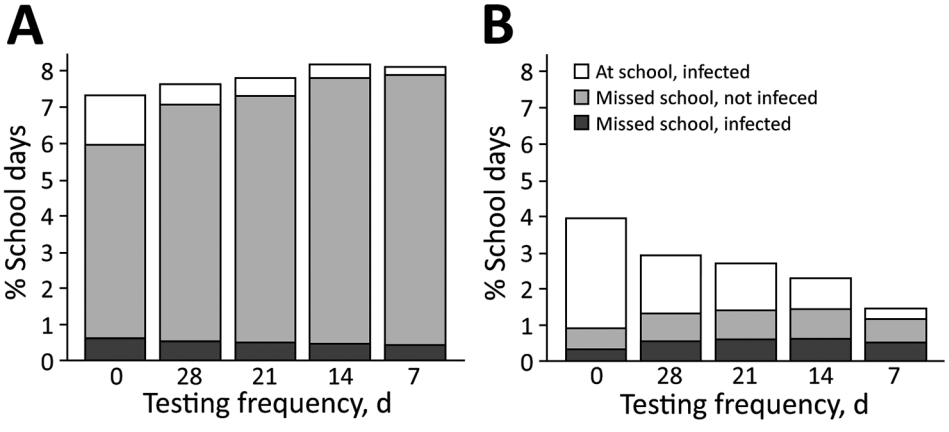

Figure 2. Projected days of school missed in a COVID-19 test allocation strategy to mitigate SARS-CoV-2 infections across 11 school districts in the Austin Independent School District, Austin, Texas, USA. The graphs demonstrate the expected proportion of school days missed due to isolation or quarantine over a 10-week period in a school with 500 students under 2 scenarios: A) assuming the household and classroom of each detected case is quarantined; or B) assuming only households (not entire classrooms) are quarantined. Estimates assume a moderate (reproduction number = 1.5) in-school transmission risk in the absence of proactive or symptomatic testing, isolation, and quarantine. All projections assume that isolation and quarantine periods last 14 days. In addition to on-campus transmission, persons might be exposed in the surrounding community at a rate of 35 new daily infections/100,000 population. The results are based on 300 stochastic simulations for each scenario.

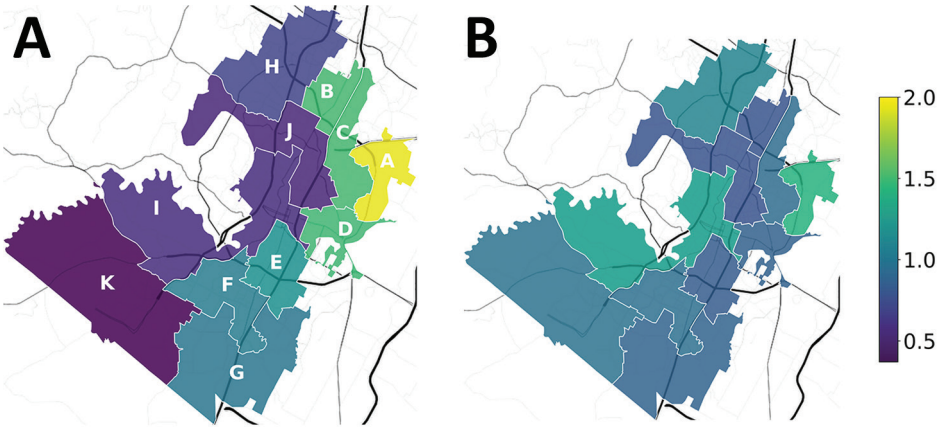

Figure 3. Locations of 11 high schools in the Austin Independent School District, Austin, Texas, USA, used to model a COVID-19 test allocation strategy to mitigate SARS-CoV-2 infections across school districts. A) Daily incidence of COVID-19 infections in late January 2021 in the catchment area of each high school relative to the average incidence across the Austin Metropolitan Statistical Area. Estimates are based on COVID-19 case reports during March 2020–January 2021. A value of one corresponds to the average incidence in the MSA. Schools are listed A through K from highest to lowest estimated daily incidence (Appendix Table 3, https://wwwnc.cdc.gov/EID/article/29/3/22-0761-App1.pdf). B) On-campus transmission risks, estimated from reported COVID-19 cases during August 16, 2020–March 8, 2021. Values are scaled so that 1.0 means that the school reported the expected number of cases, based on a least-squares linear fit of reported cases to school enrollment (Appendix Figure 4).

allocation of testing resources across schools by searching the space of possible allocations. For a given allocation, we projected the outcome for each school by first averaging the expected cumulative incidence (i.e., the mean across 300 simulations) and then the projected tail risk (i.e., the mean across the 10% worst-outcome simulations). We found the maximum value across schools (i.e., the projection for the highest-risk school) and then selected the allocation that minimized this value. Assuming that the average community incidence was 70 new daily cases per 100,000 population, based on estimates from late January 2021 in the Austin area (*42*), and that the district had a total testing budget of 1 test per student every 14 days across the district, the optimized allocation ranged from testing once per 45 days in the lowest-risk school (school K) to once per 7 days in the highest-risk school (school A) (Figure 4, panel A). We assumed that testing could not be administered more frequently than weekly. The optimal allocation

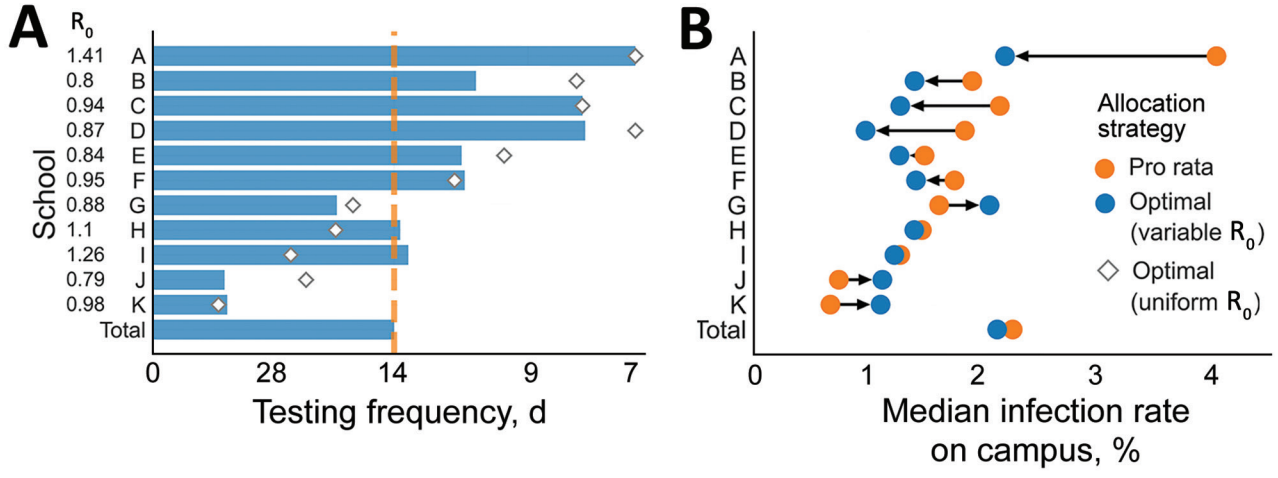

Figure 4. Test allocations and estimated infection rates based on testing frequency in a COVID-19 test allocation strategy to mitigate SARS-CoV-2 infections across 11 school districts in the Austin Independent School District, Austin, Texas, USA. A) Testing allocation for 3 testing strategies. Orange dashed line indicates pro rata strategy; blue bars indicate optimized strategy to minimize the maximum risk; diamonds indicate optimized strategy considering only variation in community transmission risks. Numbers to the left of the y-axis indicate the assumed on-campus reproduction number for each school. B) The median percent of students infected on-campus under the optimized strategy (blue) and pro rata strategy (orange), over a 10-week period; arrows indicate increases or decreases in infection rates. We modeled infections rates by using 3 testing strategies: pro rata, in which all schools test their students once per every 14 days; optimized to minimize the maximum risk of any school, considering variation in both community and in-school transmission risks; optimized considering only variation in community transmission risks. Values are averaged across 300 simulations (Appendix Table 4, https://wwwnc.cdc.gov/EID/article/29/3/22-0761-App1.pdf). The model assumes that classrooms quarantine for 14 days following a positive test.

differed slightly when we assumed instead that schools had the same on-campus R_0 and differences in risk stemmed solely from the community force of infection (Figure 4, panel A).

We projected infection rates under both the optimized allocation and a nonoptimized pro rata allocation in which resources would be allocated proportional to enrollment (Figure 4, panel A). We expected the optimized strategy to slightly reduce the overall infection rate for the district relative to the pro rata strategy and equalize risks across campuses. In the optimized strategy, the median infection rate increased by 0.4% for the lowest-risk school (school K) and decreased by 1.8% for the highest-risk school (school A) (Appendix Table 4).

When we considered total incidence by combining both community-acquired and school-acquired infections, we expected ≈5.8-fold difference between the highest risk and lowest risk schools, in the absence of testing (Figure 5, panel A). Using a 14-day testing budget, we found a pro rata strategy would lower overall incidence but not reduce the disparity (Figure 5, panel B), but an optimized allocation would greatly shrink the gap to a 3.6-fold difference (Figure 5, panel C). Restricting our analysis to infections that occur on campus, the optimized allocation again reduced the disparity in risk across schools (Table).

To provide intuition, we also derived an optimal testing allocation to reduce risks in a hypothetical district containing 6 schools, 1 of each combination of either low or high external risk and either low, moderate, or high internal risk (Appendix Figures 8, 9). We compared 3 possible testing scenarios: no testing, universal testing every 2 weeks, and an optimal testing strategy in which the 2-week testing budget is allocated to schools to minimize the maximum risk experienced by any school in the system. We found that going from no testing to a pro rata allocation decreased the maximum risk for any school from 24.7% (95% CI 11.9–38.0) of students infected to 6.6% (95% CI 3.0–11.4); under the optimal allocation, risk was further reduced to 4.5% (95% CI 1.4–8.3). Using this strategy, the total expected risk across all 6 schools was reduced from 12.8% (95% CI 9.0–16.9) of infections without testing to 3.8% (95% CI 2.5–5.2) with a pro rata allocation, which was further reduced to 3.5% (95% CI 2.4–4.8) under the optimal testing allocation (Appendix Figure 14, panel B).

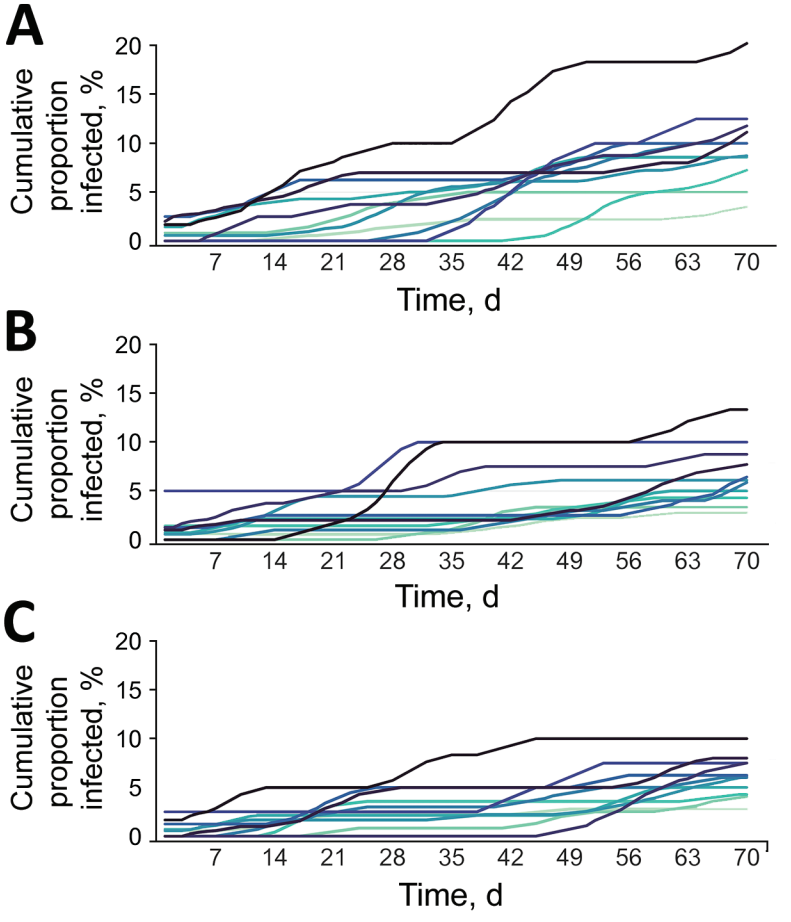

Figure 5. Cumulative infections in schools used to model a COVID-19 test allocation strategy to mitigate SARS-CoV-2 infections across 11 school districts in the Austin Independent School District, Austin, Texas, USA. Graphs represent cumulative COVID-19 infections over a 10-week period under 3 testing scenarios: A) no testing; B) all schools test students every 14 days; and C) optimized allocation of tests based on school-specific transmission risks, assuming a district-wide budget of 1 test per student every 14 days. Schools are ordered from A–K based on community incidence from high to low in the school catchment area. Graphs show 7-day moving averages based on a single simulation for each scenario and school. To show representative projections, we selected the simulation that produced a cumulative attack rate closest to the median across all 300 simulations.

Table. Estimated heterogeneity in COVID-19 incidence and total disease burden across 11 high schools in the Austin Independent School District, Austin, Texas, USA, under 3 testing scenarios in a modeled COVID-19 test allocation strategy to mitigate SARS-CoV-2 infections across school districts*

Infections	Testing allocation		
	No testing	Pro rata testing	Optimal testing
Total infections†			
Risk gap	5.8	4.8	3.6
Gini coefficient (SE)‡	0.23 (0.053)	0.26 (0.057)	0.19 (0.037)
No. infections (95% CI)§	115 (79–158)	70 (50–94)	69 (49–93)
Infection rate (95% CI)§	9.4 (6.5–12.9)	5.7 (4.1–7.7)	5.6 (4–7.6)
On-campus infections#			
Risk gap	6.5	5.6	1.8
Gini coefficient (SE)‡	0.27 (0.098)	0.23 (0.075)	0.13 (0.041)
No. infections (95% CI)§	70 (38–119)	27 (13–49)	26 (12–48)
Infection rate (95% CI)§	5.8 (3.1–9.7)	2.2 (1.1–4.1)	2.1 (1.0–3.9)

*The risk gap is the ratio of the median cumulative incidence across 300 simulations of the school with the highest expected incidence to that of the school with the lowest expected incidence.
†Total student infections, occurring both on and off campus, over the 10-week projection period.
‡Gini coefficients indicate overall disparities in expected burden, where values of 0 correspond to maximum equality and values of 1 correspond to maximum inequality (*43*). Gini coefficients were calculated using the median proportion of students infected across 300 simulations.
§The total median infections in the district over the horizon simulated, expressed as absolute and per capita.
#Infections occurring on campus, over the 10-week projection period.

Discussion

Proactive testing can be an effective strategy for preventing SARS-CoV-2 transmission on school campuses, if test turnaround is short and positive cases are immediately isolated (*44*; A. Bilinski, unpub. data, https://doi.org/10.1101/2021.05.12.21257131).Because testing requires considerable time, resources, and personnel, schools might opt to streamline their efforts as COVID-19 risks change. Our study provides a framework to help school districts allocate limited testing resources across different schools, depending on the in-school and local community transmission risks, while weighing the costs and benefits of classroom quarantine after a positive test. Prioritizing testing based on estimated risks can help mitigate the disproportionate COVID-19 burden falling on lower socioeconomic and racial minority neighborhoods (*45*–*47*).

Our results suggest that the optimal allocation of tests across schools depends on both the in-school transmission rate and the force of infection from the surrounding community. However, estimating in-school risks is difficult without sufficient testing because of overdispersion in the distribution of secondary cases and the small proportion of children that develop symptoms upon SARS-CoV-2 infection (*48*). A modest level of baseline surveillance testing could help determine the relative risks across schools (*49*). Our case study of AISD high schools suggests that even without such information, allocating testing resources based on community risks alone could substantially close gaps among schools (Appendix Figure 7).

Although proactive testing can lower and equalize COVID-19 risks across a heterogeneous school district, disparities are likely to persist. Schools drawing from neighborhoods with high COVID-19 incidence will continue to experience higher case counts and absenteeism. Other intervention measures, including vaccination and use of face masks, are essential for further reducing risks and ensuring equitable access to education.

The optimal allocation of scarce resources across multiple entities, like the number of tests per school, depends on the state of the entire system. A school might receive anywhere from no tests to enough tests for weekly testing of every student, depending on the level of risk relative to other schools. Schools could potentially game the system to gain larger allocations. For example, a school could inflate reported cases or enable higher rates of transmission by allowing high-risk activities or relaxing precautionary measures. If such issues arose, then allocation calculations could be based solely on estimates for the force of infection from the surrounding communities.

This approach can be broadly applied to distributing limited SARS-CoV-2 testing resources across systems with heterogeneous risks, such as workplaces, correctional facilities, or long-term care facilities. Our case study demonstrates that, even within a single city, tailoring control strategies to hyperlocal estimates of risks can reduce transmission overall and mitigate chronic disparities in access to resources and disease burden. On larger geographic scales, spatiotemporal variation in COVID-19 risks has been even more apparent, and cities, states, and countries exhibit highly asynchronous waves of transmission. Dynamic allocation of scarce public health resources based on reliable estimates of risk could substantially reduce the burden of COVID-19 and future pathogen

threats across the United States but requires considerable coordination at the state and federal level.

The first limitation of our study is that we assumed immediate in-school and community risks could be reliably estimated. In practice, the data required to estimate such risks often lag, are biased, or are unavailable. Such uncertainty could be included in our model by using stochastic variables that evolve based on test results from each school. However, the additional complexity would slow computational optimization. Second, we estimated heterogeneity in incidence but did not explicitly consider vaccination, health outcomes other than incidence, or socioeconomic or other factors known to correlate with COVID-19 risks (*50*). Schools drawing from more vulnerable communities might have access to fewer mitigation resources besides testing, lower vaccination coverage, or higher infection hospitalization and mortality rates. Such factors could be explicitly modeled and incorporated into the objective function used to derive equitable allocations. Third, the study derived allocations to minimize infections occurring across a school district. However, other outcomes could be explicitly incorporated into further analyses, including absenteeism and loss of education resulting from isolation and quarantine. The costs and benefits of quarantining entire classrooms, in addition to the households of positive cases, depend on the frequency of testing. Classroom quarantine would always be expected to elevate absenteeism but only substantially reduces exposure risks when testing is infrequent. With frequent testing or low transmission risks, limiting the scope and duration of quarantine might be advisable. Hospitalization risks for school staff and the potential for schools to exacerbate transmission in the surrounding community also could be integrated into allocation calculations. Finally, our model does not consider the potential costs or logistical impediments to dynamically allocating tests among schools. In addition to the challenges of rapidly calculating allocations and distributing tests accordingly, schools might require additional trained staff to administer tests, conduct contact tracing, and ensure the quick and safe isolation and quarantine of affected persons (*30*).

In conclusion, as the United States plans for COVID-19 postpandemic management, proactive testing will remain a highly effective countermeasure that can be tailored to changing risks on a local scale. As tests become more economical and as surveillance within schools and communities improves, our model demonstrates that school systems can optimize testing and quarantine policies to prevent transmission, limit absenteeism, and ensure continuity of operations during future COVID-19 surges.

Acknowledgments

We thank the Texas Advanced Computing Center at The University of Texas (Austin, TX, USA) for providing high performance computing and database resources that contributed to the research results.

This work was supported by grant no. U01IP001136 from the Centers for Disease Control and Prevention, grant no. NIH-R01-AI151176 from the National Institutes of Health, grant no. 17STQAC00001-04-00US from the Department of Homeland Security, and a generous donation from Tito's Handmade Vodka. The funders had no role in the design and conduct of the study; collection, management, analysis, and interpretation of the data; preparation, review, or approval of the manuscript; or decision to submit the manuscript for publication. The views and conclusions contained in this document are those of the authors and should not be interpreted as necessarily representing the official policies, either expressed or implied, of the funding institutions.

About the Author

Mr. Pasco is a PhD candidate at the University of Texas at Austin, Austin, Texas, USA. His research interests include mathematical modeling of infectious diseases and operations research.

References

1. Johns Hopkins Coronavirus Resource Center. COVID-19 map [cited 2023 Jan 13]. https://coronavirus.jhu.edu/map.html
2. United Nations Conference on Trade and Development. COVID-19's economic fallout will long outlive the health crisis, report warns [cited 2021 Apr 13]. https://unctad.org/news/covid-19s-economic-fallout-will-long-outlive-health-crisis-report-warns
3. Czeisler MÉ, Lane RI, Petrosky E, Wiley JF, Christensen A, Njai R, et al. Mental health, substance use, and suicidal ideation during the COVID-19 pandemic—United States, June 24–30, 2020. MMWR Morb Mortal Wkly Rep. 2020; 69:1049–57. https://doi.org/10.15585/mmwr.mm6932a1
4. Vahratian A, Blumberg SJ, Terlizzi EP, Schiller JS. Symptoms of anxiety or depressive disorder and use of mental health care among adults during the COVID-19 pandemic—United States, August 2020–February 2021. MMWR Morb Mortal Wkly Rep. 2021;70:490–4. https://doi.org/10.15585/mmwr.mm7013e2
5. Center on Budget and Policy Priorities. Tracking the COVID-19 recession's effects on food, housing, and employment hardships [cited 2021 Apr 13]. https://www.cbpp.org/research/poverty-and-inequality/tracking-the-covid-19-recessions-effects-on-food-housing-and
6. Parker K, Minkin R, Bennett J. Economic fallout from COVID-19 continues to hit lower-income Americans the hardest. Pew Research Foundation; 2020 Sep 24 [cited 2021 Apr 13]. https://www.pewresearch.org/social-trends/2020/09/24/economic-fallout-from-covid-19-continues-to-hit-lower-income-americans-the-hardest

7. Azevedo JP, Hasan A, Goldemberg D, Geven K, Iqbal SA. Simulating the potential impacts of COVID-19 school closures on schooling and learning outcomes: a set of global estimates [cited 2021 Apr 13]. World Bank Res Obs. 2021;36:1–40. https://academic.oup.com/wbro/article-pdf/36/1/1/36757308/lkab003.pdf.
8. Engzell P, Frey A, Verhagen MD. Learning loss due to school closures during the COVID-19 pandemic. Proc Natl Acad Sci U S A. 2021;118:e2022376118. https://doi.org/10.1073/pnas.2022376118
9. Dorn E, Hancock B, Sarakatsannis J, Viruleg E. COVID-19 and learning loss—disparities grow and students need help. McKinsey & Company. 2020 [cited 2021 Apr 13]. https://www.mckinsey.com/industries/public-and-social-sector/our-insights/covid-19-and-learning-loss-disparities-grow-and-students-need-help
10. Baron EJ, Goldstein EG, Wallace CT. Suffering in silence: How COVID-19 school closures inhibit the reporting of child maltreatment. J Public Econ. 2020;190:104258. https://doi.org/10.1016/j.jpubeco.2020.104258
11. Kinsey EW, Hecht AA, Dunn CG, Levi R, Read MA, Smith C, et al. School closures during COVID-19: opportunities for innovation in meal service. Am J Public Health. 2020; 110:1635–43. https://doi.org/10.2105/AJPH.2020.305875
12. Orgilés M, Morales A, Delvecchio E, Mazzeschi C, Espada JP. Immediate psychological effects of the COVID-19 quarantine in youth from Italy and Spain. Front Psychol. 2020;11:579038. https://doi.org/10.3389/fpsyg.2020.579038
13. Honein MA, Barrios LC, Brooks JT. Data and policy to guide opening schools safely to limit the spread of SARS-CoV-2 infection. JAMA. 2021;325:823–4. https://doi.org/10.1001/jama.2021.0374
14. Education Week Staff. A year of COVID-19: what it looked like for schools. Education Week. 2021 Mar 4 [cited 2021 Nov 2]. https://www.edweek.org/leadership/a-year-of-covid-19-what-it-looked-like-for-schools/2021/03
15. Center for American Progress. Remote learning and school reopenings: what worked and what didn't [cited 2021 Nov 2]. https://www.americanprogress.org/issues/education-k-12/reports/2021/07/06/501221/remote-learning-school-reopenings-worked-didnt
16. US Centers for Disease Control and Prevention. COVID data tracker [cited 2021 Aug 12]. https://covid.cdc.gov/covid-data-tracker/#vaccinations_vacc-total-admin-rate-total
17. Busser C. NEA survey finds educators back in classrooms and ready for fall. National Education Association. 2021 Jun 17 [cited 2021 Nov 2]. https://www.nea.org/about-nea/media-center/press-releases/nea-survey-finds-educators-back-classrooms-and-ready-fall
18. Gutman-Wei R. Why is it taking so long to get vaccines for kids? The Atlantic. 2021 Aug 11 [cited 2021 Aug 12]. https://www.theatlantic.com/health/archive/2021/08/covid-vaccination-timeline-children/619729/
19. US Food and Drug Administration. FDA Authorizes Pfizer-BioNTech COVID-19 vaccine for emergency use in children 5 through 11 years of age [cited 2021 Dec 6]. https://www.fda.gov/news-events/press-announcements/fda-authorizes-pfizer-biontech-covid-19-vaccine-emergency-use-children-5-through-11-years-age
20. Goldstein D. Omicron upends return to school in U.S. The New York Times. 2022 Jan 3 [cited 2022 Jan 5]. https://www.nytimes.com/live/2022/01/03/us/school-closings-covid
21. Parks SE, Zviedrite N, Budzyn SE, Panaggio MJ, Raible E, Papazian M, et al. COVID-19–related school closures and learning modality changes—United States, August 1–September 17, 2021. MMWR Morb Mortal Wkly Rep. 2021;70:1374–6. https://doi.org/10.15585/mmwr.mm7039e2
22. US Department of Health and Human Services. Biden administration to invest more than $12 billion to expand COVID-19 testing [cited 2021 Jul 7]. https://www.hhs.gov/about/news/2021/03/17/biden-administration-invest-more-than-12-billion-expand-covid-19-testing.html
23. US Department of Education. Department of Education announces American Rescue Plan funds for all 50 States, Puerto Rico, and the District of Columbia to help schools reopen [cited 2021 Jul 5]. https://www.ed.gov/news/press-releases/department-education-announces-american-rescue-plan-funds-all-50-states-puerto-rico-and-district-columbia-help-schools-reopen
24. Larremore DB, Wilder B, Lester E, Shehata S, Burke JM, Hay JA, et al. Test sensitivity is secondary to frequency and turnaround time for COVID-19 screening. Sci Adv. 2021;7:eabd5393. https://doi.org/10.1126/sciadv.abd5393
25. Du Z, Pandey A, Bai Y, Fitzpatrick MC, Chinazzi M, Pastore Y Piontti A, et al. Comparative cost-effectiveness of SARS-CoV-2 testing strategies in the USA: a modelling study. Lancet Public Health. 2021;6:e184–91. https://doi.org/10.1016/S2468-2667(21)00002-5
26. Paltiel AD, Zheng A, Walensky RP. Assessment of SARS-CoV-2 screening strategies to permit the safe reopening of college campuses in the United States. JAMA Netw Open. 2020;3:e2016818. https://doi.org/10.1001/jamanetworkopen.2020.16818
27. Lanier WA, Babitz KD, Collingwood A, Graul MF, Dickson S, Cunningham L, et al. COVID-19 testing to sustain in-person instruction and extracurricular activities in high schools—Utah, November 2020–March 2021. MMWR Morb Mortal Wkly Rep. 2021;70:785–91. https://doi.org/10.15585/mmwr.mm7021e2
28. Frazier PI, Cashore JM, Duan N, Henderson SG, Janmohamed A, Liu B, et al. Modeling for COVID-19 college reopening decisions: Cornell, a case study. Proc Natl Acad Sci U S A. 2022;119:e2112532119. https://doi.org/10.1073/pnas.2112532119
29. Vohra D, Rowan P, Goyal R, Hotchkiss J, O'Neil S. Early insights and recommendations for implementing a covid-19 antigen testing program in K-12 schools: lessons learned from six pilot sites. New York: The Rockefeller Foundation; 2021 [cited 2021 Apr 13]. https://www.rockefellerfoundation.org/wp-content/uploads/2021/02/Early-Insights-and-Recommendations-for-K-12-Schools-Covid-19-Testing-Lessons-Learned-from-Six-Pilot-Sites.pdf
30. Faherty LJ, Master BK, Steiner ED, Kaufman JH, Predmore Z, Stelitano L, et al. COVID-19 testing in K-12 schools–insights from early adopters. Santa Monica (CA): RAND Corporation; 2021 [cited 2021 Jul 5]. https://www.rockefellerfoundation.org/wp-content/uploads/2021/02/RAND_Covid-19-Testing-in-K-12-Schools_Insights-from-Early-Adopters.pdf
31. Howard J. Debate emerges around Covid-19 testing strategies in schools as districts plan to reopen. CNN. 2021 Jul 19 [cited 2021 Nov 2]. https://www.cnn.com/videos/tv/2021/07/19/lead-erica-hill-live-jake-tapper.cnn
32. Austin Independent School District. About our schools [cited 2021 May 19]. https://www.austinisd.org/schools
33. Austin Independent School District. COVID-19 dashboard [cited 2021 Apr 14]. https://www.austinisd.org/openforlearning/dashboard
34. Abbott. Taking COVID-19 testing to a new level [cited 2021 Apr 14]. https://www.abbott.com/BinaxNOW-Test-NAVICA-App.html

35. Davies NG, Klepac P, Liu Y, Prem K, Jit M, Eggo RM; CMMID COVID-19 working group. Age-dependent effects in the transmission and control of COVID-19 epidemics. Nat Med. 2020;26:1205–11. https://doi.org/10.1038/s41591-020-0962-9
36. Gudbjartsson DF, Helgason A, Jonsson H, Magnusson OT, Melsted P, Norddahl GL, et al. Spread of SARS-CoV-2 in the Icelandic population. N Engl J Med. 2020;382:2302–15. https://doi.org/10.1056/NEJMoa2006100
37. Pollock NR, Jacobs JR, Tran K, Cranston AE, Smith S, O'Kane CY, et al. Performance and implementation evaluation of the Abbott BinaxNOW Rapid Antigen Test in a high-throughput drive-through community testing site in Massachusetts. J Clin Microbiol. 2021;59:e00083-21. https://doi.org/10.1128/JCM.00083-21
38. US Food and Drug Administration. Abbott BinaxNOW COVID-19 Ag CARD instructions for use and characteristics [cited 2021 Apr 19]. https://www.fda.gov/media/141570/download
39. He X, Lau EHY, Wu P, Deng X, Wang J, Hao X, et al. Temporal dynamics in viral shedding and transmissibility of COVID-19. Nat Med. 2020;26:672–5. https://doi.org/10.1038/s41591-020-0869-5
40. He D, Zhao S, Lin Q, Zhuang Z, Cao P, Wang MH, et al. The relative transmissibility of asymptomatic COVID-19 infections among close contacts. Int J Infect Dis. 2020;94:145–7. https://doi.org/10.1016/j.ijid.2020.04.034
41. University of Texas at Austin COVID-19 Modeling Consortium. Heterogeneous burden of the COVID-19 pandemic in central Texas [cited 2021 Apr 25]. https://sites.cns.utexas.edu/sites/default/files/cid/files/austin_covid-19_spatial_burden_report.pdf
42. University of Texas at Austin COVID-19 Modeling Consortium. Austin dashboard [cited 2021 Nov 5]. https://covid-19.tacc.utexas.edu/dashboards/austin
43. Atkinson AB. On the measurement of inequality. J Econ Theory. 1970;2:244–63. https://doi.org/10.1016/0022-0531(70)90039-6
44. Liu Q-H, Zhang J, Peng C, Litvinova M, Huang S, Poletti P, et al. Model-based evaluation of alternative reactive class closure strategies against COVID-19. Nat Commun. 2022;13:322. https://doi.org/10.1038/s41467-021-27939-5
45. Rubin-Miller L, Alban C, Artiga S, Sullivan S. COVID-19 Racial Disparities in Testing, Infection, Hospitalization, and Death: Analysis of Epic Patient Data. Kaiser Family Foundation; 2020 Sep 15 [cited 2021 Jul 5]. https://www.kff.org/coronavirus-covid-19/issue-brief/covid-19-racial-disparities-testing-infection-hospitalization-death-analysis-epic-patient-data
46. Mena GE, Martinez PP, Mahmud AS, Marquet PA, Buckee CO, Santillana M. Socioeconomic status determines COVID-19 incidence and related mortality in Santiago, Chile. Science. 2021;372:eabg5298. https://doi.org/10.1126/science.abg5298
47. Martin CA, Jenkins DR, Minhas JS, Gray LJ, Tang J, Williams C, et al.; Leicester COVID-19 consortium. Socio-demographic heterogeneity in the prevalence of COVID-19 during lockdown is associated with ethnicity and household size: results from an observational cohort study. EClinicalMedicine. 2020;25:100466. https://doi.org/10.1016/j.eclinm.2020.100466
48. Endo A, Abbott S, Kucharski AJ, Funk S; Centre for the Mathematical Modelling of Infectious Diseases COVID-19 Working Group. Estimating the overdispersion in COVID-19 transmission using outbreak sizes outside China. Wellcome Open Res. 2020;5:67. https://doi.org/10.12688/wellcomeopenres.15842.3
49. Leng T, Hill EM, Holmes A, Southall E, Thompson RN, Tildesley MJ, et al. Quantifying pupil-to-pupil SARS-CoV-2 transmission and the impact of lateral flow testing in English secondary schools. Nat Commun. 2022;13:1106. https://doi.org/10.1038/s41467-022-28731-9
50. Woody S, Javan E, Johnson K, Pasco R, Johnson-León M, Lachmann M, et al. Spatial distribution of COVID-19 infections and vaccinations in Austin, Texas. University of Texas at Austin. 2021 [cited 2021 Jul 5]. https://covid-19.tacc.utexas.edu/media/filer_public/fe/f2/fef289f8-800c-4390-ab27-6eff3b229f59/covid_infections_and_vaccinations_-_austin_zip_codes_-_ut_-_041221.pdf

Address for correspondence: Lauren Ancel Meyers, Department of Integrative Biology, 1 University Station C0990, Austin, TX 78712, USA; email: laurenmeyers@austin.utexas.edu

Article DOI: https://doi.org/10.3201/eid2903.220761

COVID-19 Test Allocation Strategy to Mitigate SARS-CoV-2 Infections across School Districts

Appendix

1. Transmission Model

We developed an agent-based model of COVID-19 transmission in schools, where we explicitly model interactions between students and adults working in the school environment during school days. We also include students' households in our simulation while broader community interactions are modeled through random daily introductions of new cases. In our hypothetical examples we consider schools with 500 students spread across 25 classrooms, with 25 teachers, 25 bus drivers, and 16 other school staff. The entire framework, both the transmission and the optimization models, were implemented in Python version 3.8.8 (Python Software Foundation, https://www.python.org).

1.1. Contact Structure

On weekdays students go to school and we explicitly model contacts from 7:30 AM to 3:30 PM, with contacts modeled to reflect COVID-19 precautions to limit mixing across classrooms. We model contacts in half-hour intervals in three different school contexts: (i) students commuting to and from school on the bus, (ii) classrooms, and (iii) breaks with school-wide interactions (Appendix Table 1). We did not include more elaborate contact patterns that have been analyzed in other studies (*1*; A. Bilinski, unpub. Data, https://doi.org/10.1101/2021.05.12.21257131).

We assumed that adults working at schools can be infected by students, but not by other adults. Given the relatively small number of adults working in schools and their presumed higher levels of compliance with precautionary measures, incorporating adult-to-adult transmission would only slightly increase the transmission rate.

Classroom

Each classroom is composed of 20 students and a single teacher. Students and teachers are assigned to a classroom at the beginning of the simulation and remain in the same room throughout the simulation. Therefore, each student interacts with 19 other students, as well as the same teacher, while in the classroom. Students spend 6 hours a day in the classroom.

Bus

All students commute to and from school by taking a bus. Each bus transports the same 20 students throughout the simulation and is driven by the same driver, and students are randomly assigned to a bus, independently of the classroom to which they belong. Therefore, each student interacts with 19 other students as well as the same driver while on the bus. Students spend 1 hour on the bus each day, half an hour at the beginning and at the end of the day.

Break

During the noon break students interact with other students throughout the school in cliques of 10 students; in addition, each student interacts with two adults randomly selected from the teachers and staff. The cliques of students, as well the two adults each student interacts with, are randomly determined independently of classrooms and buses, and remain constant throughout the simulation. Therefore, each student interacts with 9 other students as well as two adults while on break. Students spend 1 hour on break each day (Appendix Table 1).

Outside of school, students interact with the adults in their households. The number of adults in each student's household is determined according to data collected by the US Census Bureau regarding living arrangements of children under age 18 (*2*). For simplicity, we do not explicitly model siblings within households who attend the same school. Household transmission between such siblings can amplify school-based outbreaks if siblings who are infected at home return to school while infectious. However, the household attack rate of 16.6% (*3*), and the limited number of sibling pairs in different classrooms (*4*), would make such occurrences relatively small. In addition, the baseline quarantine strategy of quarantining an entire individual's household upon a positive test would prevent some of those sibling infections from spreading further in school.

Rather than explicitly modeling contacts within households, we use a published estimate of the household attack rate of COVID-19 and assumed infected individuals, whether adults or children, symptomatic or not, transmit the disease to 16.6% of their susceptible household (*3*). The exact time of infection is determined randomly based on the relative infectiousness of an individual through time (details below).

All interactions with the broader community are abstracted and included through a single daily community incidence value that is kept constant throughout the simulation. We determined the number of new infections due to community interactions through a binomial process. For instance, if we denote the daily community incidence of COVID-19 by p, e.g., $p = 70$ new daily cases per 100,000 population, then the number of newly infected individuals in a group with N individuals is sampled from a binomial distribution as $Binomial(N,p)$.

To account for time spent in school, the daily incidence of new cases among members of the school environment on weekdays is half that of the community, but incidence is the same on weekends.

1.2. COVID-19 Natural History

The natural history of COVID-19 is modeled according to the diagram shown in Appendix Figure 1. Infected individuals move to the exposed compartment (E) before progressing to either a presymptomatic (PY) or pre-asymptomatic (PA) compartment, from which they then move to the symptomatic infectious (IY) and asymptomatic infectious (IA) compartments, respectively. From there all infected individuals recover (R) and become immune to the disease. The transition times from one compartment to another are determined at the time of infection and follow the probability distributions listed in Appendix Table 2.

The infectiousness of all individuals varies through time, and given the average sojourn times in each compartment, the infectiousness profile follows a gamma distribution with shape and scale parameters of 2.0 and 1.55, shifted left by 2.3 days. The resulting profile is shown in blue in Appendix Figure 2, and based on the time of its maximum value (mode) this results in peak infectiousness of ≈0.7 day before symptom onset, with 45% of total infectiousness for an individual occurring in the pre-(a)symptomatic compartment, following the results from He et al. (*5*). The curve is normalized so the average infectiousness is 1.0.

As the time spent in each compartment by different individuals is randomly sampled from the probability distributions listed in Appendix Table 2, the infectiousness profile in blue in Appendix Figure 2 is adjusted for the specific time spent by an individual in the pre-(a)symptomatic and (a)symptomatic compartments using the standard times of symptom onset (or transition to infectious asymptomatic compartment), start of infectiousness (transition of pre-(a)symptomatic compartment), and recovery as the control points. For instance, individual 1 shown in green in Appendix Figure 2 spends less time in the pre-symptomatic compartment than average so the green curve before time 0 has the same shape as the blue one, but is compacted from 2.3 days to 1.8 days. Then individual 1 spends more time in the symptomatic compartment than average, so the green curve after time 0 has the same shape as the blue curve, but it is stretched to 10 days.

In addition, individuals who remain asymptomatic are assumed to be two-thirds as infectious as symptomatic persons at any given point (*6*), with 20% of children and 57% of adults becoming symptomatic (*7*,*8*).

1.3. Infection Events Modeling

When an infected individual indexed by j interacts with a susceptible individual indexed by k at time t in school for one time step of half an hour, the probability that j infects k is given by:

$$q_t = \beta \cdot \omega_j \cdot i_j(t)$$

where $\omega_j = 1.0$ if individual j is symptomatic or pre-symptomatic and $\omega_j = 2/3$ if individual j is asymptomatic or pre-asymptomatic; here, $i_j(t)$ represents the relative infectiousness of individual j at time t as shown in Appendix Figure 2, and β is an input parameter that is selected so that the unmitigated reproduction number R_0 of children in school is equal to a chosen input. It represents the probability that a symptomatic individual with relative infectiousness of 1.0 at time t infects a susceptible contact in a half-hour interval.

We use the following to determine β:

$d_I = d_P + d_S$ the total infectious period in days, which is the sum of the pre-(a)symptomatic and (a)symptomatic periods

τ proportion of symptomatic students

h_x, C_x the number of hours spent in school context x (of the 3 contexts detailed above) and the number of contacts in that context

$\omega_a = 2/3$, $\omega_s = 1$ scaling factor of the relative infectiousness of asymptomatic and symptomatic individuals through their infection $\Delta t = 1/2$-hour single time step duration in the simulations

We can calculate the desired R_0 in school as the sum of R_0 in the three different school contexts: $R_0 = R_0(\text{class}) + R_0(\text{bus}) + R_0(\text{break})$.

The basic reproduction number in a given place is simply the probability of infecting a given contact multiplied by the number of contacts: $R_0(x) = C_x \cdot p(x)$, where $p(x)$ represents the probability of infecting a single individual contact in context x over the individual's entire infectious period. Then:

$$R_0 = p(class) \cdot C_{class} + p(bus) \cdot C_{bus} + p(break) \cdot C_{break}$$

$$R_0 = p(class) \cdot [C_{class} + \frac{1}{h_{class}}(C_{bus} \cdot h_{bus} + C_{break} \cdot h_{break})]$$

where we make the simplification that the probability of infecting an individual is directly proportional to the total time spent in contact with them.

We now only need to calculate the probability of infecting an individual who is a classroom contact, $p(class)$. This probability is averaged over symptomatic and asymptomatic individuals. To simplify calculations, we calculated the probability that a symptomatic individual would infect another person in their classroom, $p(class)$, with subscript s to denote symptomatic, which is given by:

$$p_s(class) \cdot [\tau + \omega_s + (1 - \tau) \cdot \omega_a)] = p(class).$$

We can then write the relationship between the probability of a symptomatic infectious individual infecting a contact at some point in time, with the probability of infection at each time step in the simulation via:

$$1 - p_s(class) = \prod_{t=t_0}^{T}(1 - q_t)$$

By definition, for a symptomatic individual we have $q_t = \beta \cdot i_j(t)$, which depends on t through the individual's relative infectiousness. We simplify this by $q_t = \beta$ using the fact that $i_j(t)$ is constructed to have an average value of 1. As a result, we have the following:

$$1 - p_s(class) = \prod_{t=t_0}^{T} (1 - \beta) = (1 - \beta)^N$$

where N represents the average number of time steps that an infected individual has with other contacts in their classroom while infectious:

$$N = \frac{h_{class}}{\Delta t} \cdot d_I \cdot \frac{5}{7}$$

and we use 5/7 to represent the fact that school days occur on weekdays only.

Finally, we obtain

$$\beta = 1 - [1 - p_s(class)]^{\frac{1}{N}}.$$

1.4. Testing and Isolation

In all scenarios, we assumed that 90% of symptomatic individuals will seek testing once symptoms occur. The exact time after symptom onset at which individuals seek testing is random and is sampled from a triangular distribution with an average of 1 day, a lower bound of 0.5 day, and an upper bound of 1.5 day. We assume that the tests that symptomatic individuals use are perfect, and separate from the surveillance testing budget. In addition, 2 hours after getting tested, the symptomatic individual starts their isolation, and if applicable their contacts quarantine themselves at the same time. For surveillance testing the results are assumed to be instantaneous. The infected individual then starts their isolation immediately, and their contacts quarantine themselves immediately as well. In the baseline scenarios all isolations and quarantines last 14 days, according to the Austin Independent School District (AISD) policy during the 2020–2021 school year (*9*).

In our simulation, surveillance tests are all done on Mondays at 8 AM, right after students take the bus to school and before the first class. If students are isolated or quarantined for 2 weeks, they come back to school on the second Monday after testing positive.

In addition, surveillance tests are allocated across classrooms every week. For instance, if 50% of a school's students are tested every week, then 50% of the students in each classroom are

tested each week, according to a defined schedule so that every student will be tested every other week. This method of test allocation within a school performed better in our experiments than randomly selecting the students for testing, or testing entire classrooms some weeks while no student is tested in other classrooms.

We assumed that individuals strictly quarantine themselves, so that they cannot be infected with contacts from the broader community. However, in this case, students could still be infected by one of their household members.

In our base-case scenario, we assumed that surveillance tests were perfect, but we ran some sensitivity analysis relaxing this assumption. We ran some scenarios where the tests had a sensitivity of 95% for symptomatic individuals, 80% for pre-(a)symptomatic and asymptomatic individuals, and a 99% specificity, which corresponds to pre-Delta estimates published for the Abbott BinaxNOW tests (*10*,*11*). Parameters are provided in Appendix Table 2.

2. Optimization Model

We optimize the allocation of tests across a set of schools to minimize a chosen risk metric. The results shown in the main text seek to minimize the maximum risk across schools and the associated model is presented in the following section. We have explored other objective functions, and we show the corresponding model formulations in this section as well as the resulting allocations as a sensitivity analysis further below.

As part of our optimization model formulation, we use the preprocessed results from the simulation model above as inputs, so the optimization part of the framework is run independently and subsequently to the disease transmission model.

2.1. Notation

Set and indices: $s \in S$ set of schools in the system.

Parameters: N_s number of students in school s; B testing budget, expressed as the proportion of students in the entire system that can be tested weekly.

Variables: t_s proportion of students tested each week in school s; $I_s(t_s)$ proportion of students in school s infected on-campus over the horizon under testing regime t_s.

The decision variable t_s represents the testing regimen in a school and is expressed as the proportion of the school's students tested each week. For example, $t_s = 50\%$ means that every week 50% of the school's students are screened so that, on average, students get tested every other week, while with $t_s = 33\%$ students are tested every 3 weeks on average. Evaluating $I_s(t_s)$ requires running the simulation model of disease transmission that we sketch above for 300 simulations, given a specific value of t_s.

2.2. Model

The objective of the optimization model is to minimize the maximum risk experienced by any school in the system subject to two constraints.

First, we cannot allocate more tests than are available in the budget:

$$\sum_{s \in S} N_s \cdot t_s \leq B \cdot \sum_{s \in S} N_s \qquad [C1]$$

Second, we limit testing to a weekly frequency in each school:

$$0 \leq t_s \leq 1, \forall s \in S \qquad [C2]$$

The risk metric we aim to minimize is the average of (i) the on-campus expected infection rate across simulations $\mathrm{E}\{I_s(t_s)\}$, and (ii) the conditional value-at-risk (CVaR) of the infection rate at a level $\beta = 90\%$, $CVaR_{90}\{I_s(t_s)\}$. Therefore, the risk for school s given a testing regimen t_s is

$$R_s(t_s) = \frac{1}{2}[\mathbb{E}\{I_s(t_s)\} + CVaR_{90}\{I_s(t_s)\}].$$

CVaR, also called expected shortfall, is a widely used risk measure in stochastic optimization, thanks to its coherence properties, ease of interpretation, and computational tractability (*13*,*14*). Consider a random variable, X, that we would like to keep "small," such as the proportion of a population that is infected with COVID-19. CVaR is the conditional expectation given that X exceeds its β-level quantile. Thus, in our case, with $\beta = 0.90$, $CVaR_{90}\{I_s(t_s)\}$ computes the conditional expectation of the worst 10% of the outcomes, or the average proportion of infected students at a school, when restricting that average to the 30 simulated scenarios out of 300 with the largest proportion of infections. Hence, including this term helps determine a test-allocation strategy that controls tail risk. Formally, for a random

variable X with cumulative distribution function $F(x)$, value-at-risk (VaR) and CVaR are defined as follows:

$$VaR_\beta(X) = \inf\{x : F(x) \geq \beta\} = F^{-1}(\beta)$$
$$CVaR_\beta(X) = \mathbb{E}\{X | X \geq VaR_\beta(X)\}.$$

Then the optimization problem can be expressed as the following:

$$\min_{t_s} \max_{s \in S} R_s(t_s)$$
$$s.t. [C1], [C2]$$

Put together and reformulated, this gives us the following optimization model, where the decision variables are the various amounts of testing t_s in each school:

$$(P) \quad \begin{aligned} \min \quad & z \\ s.t. \quad & \frac{1}{2}\left[\mathbb{E}\{I_s(t_s)\} + CVaR_{90}\{I_s(t_s)\}\right] \leq z, \quad \forall s \in S \\ & \sum_{s \in S} N_s \cdot t_s \leq B \cdot \sum_{s \in S} N_s \\ & 0 \leq t_s \leq 1, \quad \forall s \in S \end{aligned}$$

Due to the nonlinear, and effectively black-box, nature of the functions $I_s(t_s)$ with respect to t_s and the fact that we summarize the risk of each school using the infection rate's expected value and CVaR, this is a nonlinear black-box continuous optimization problem that can be solved with standard solvers. We used the COBYLA method implemented in SciPy/Python to solve the problem (*15*,*16*).

Our optimization model is nonlinear and nonconvex but has two key properties that allow us to readily check whether a solution is globally optimal. First, the risk function associated with each school

$$R_s(t_s) = \frac{1}{2}[\mathbb{E}\{I_s(t_s)\} + CVaR_{90}\{I_s(t_s)\}]$$

is a decreasing function of the allocation t_s. Second, we are solving a continuous minimax problem in which we are focused on the school with the worst-case risk. Thus, we can first allocate resources to the worst-case school to decrease its risk to that of the school with the second-highest risk, and repeat this scheme until the budget is exhausted, dealing with obvious edge cases. This allows us to verify that the solution found via COBYLA is indeed a globally optimal solution.

Testing cannot be more frequent than weekly, i.e., $t_s \leq 1$. When solving problem (P), we may observe that some schools, indexed by say, $s \in S'$, are allocated enough tests for weekly testing. To help reduce the dimension and aid the solver in its search, we can fix the corresponding decision variables of the schools with weekly testing t_s, $s \in S'$, to 1, and rerun COBYLA to optimize the allocation for the remaining schools, excluding those schools from the first constraint in (P). The problem then becomes the following:

$$
(P') \quad \begin{aligned}
\min \quad & z \\
s.t. \quad & \frac{1}{2}\left[\mathbb{E}\{I_s(t_s)\} + CVaR_{90}\{I_s(t_s)\}\right] \leq z, \quad \forall s \in S \backslash S' \\
& \sum_{s \in S} N_s \cdot t_s \leq B \cdot \sum_{s \in S} N_s \\
& 0 \leq t_s \leq 1, \quad \forall s \in S \backslash S' \\
& t_s = 1, \quad \forall s \in S'
\end{aligned}
$$

After sketching two alternative formulations, we describe another means by which we help the optimization algorithm in terms of preprocessing output from the simulation model.

2.3. Alternative Objective Functions

Below we show the optimization model when minimizing different objective functions. In Appendix Figure 15, we show the resulting optimal allocations from solving those problems for the hypothetical school system.

Varying CVaR Level and Relative Weight

Two straightforward modifications to the original optimization problem are to change the level β of CVaR as well as the respective weights of CVaR and of the expectation in the risk level of each school. The problem is easily modified, using some value, $w \in [0,1]$ for the weight of CVaR, we have the following:

$$
(P_{w,\beta}) \quad \begin{aligned}
\min \quad & z \\
s.t. \quad & (1-w) \cdot \mathbb{E}\{I_s(t_s)\} + w \cdot CVaR_{\beta}\{I_s(t_s)\} \leq z, \quad \forall s \in S \\
& \sum_{s \in S} N_s \cdot t_s \leq B \cdot \sum_{s \in S} N_s \\
& 0 \leq t_s \leq 1, \quad \forall s \in S
\end{aligned}
$$

By setting w to 0 or 1 we can focus either on the expected infection rate or on the CVaR of infection rates respectively, thus ignoring tail risk entirely or focusing solely on it.

Total Expectation

A different approach is to try to minimize total infections occurring across the entire system rather than trying to minimize the risk for the highest-risk school, as in the main text. Then the size of different schools, through the number of students N_s, directly impacts the objective function. The problem is formulated as follows:

$$(P_{total}) \quad \begin{aligned} \min \quad & \sum_{s \in S} N_s \cdot \mathbb{E}\{I_s(t_s)\} \\ s.t. \quad & \sum_{s \in S} N_s \cdot t_s \leq B \cdot \sum_{s \in S} N_s \\ & 0 \leq t_s \leq 1, \quad \forall s \in S \end{aligned}$$

2.4. Inputs Preprocessing

To run the optimization model, we need to preprocess the results from the transmission model to smooth out some of the stochasticity of the simulations. We do this in two steps.

First, we take the results from the 300 simulations for a single parameter set, which corresponds to a specific school with a certain testing frequency, and we fit a gamma distribution to the proportion of students infected on-campus (Appendix Figure 3, panel A). This ensures that the risk metrics we calculate are not biased by single simulations and that the CVaR metric stays continuous with respect to the exact level β chosen.

Second, using those fitted gamma distributions, we calculate the risk for all schools for each of the 21 testing amounts simulated, from no students tested to all students tested weekly, in 5% increments. This produces the blue dots in Appendix Figure 3, panel B. We then fit a non-increasing curve to these dots, specifically we fit a cubic curve up to the point where 75% of students are tested weekly and then a linear curve. This piecewise definition of the curve helps us keep the number of parameters necessary for fitting low enough to have a parsimonious model while having a good fit.

This process ensures that the risk level of a school decreases as the testing frequency increases, which might not always be the case in our simulations due to stochasticity, especially when the number of infections is already low. Additionally, explicitly pre-calculating the risk level of a school as a function of the testing frequency ensures rapid execution of the optimization routine because the COBYLA algorithm might require a large number of iterations when the risk level of each school must be evaluated.

3. AISD Details

The list of high schools from the Austin Independent School District (AISD) included in our analysis is given in Appendix Table 3 along with the number of students modeled in our simulations (*17*). The number of students in each school is based on enrollment reports from the Texas Education Agency (TEA) multiplied by the reported in-person attendance of 6% in AISD high schools at the beginning of January 2021 (*18*,*19*). We rounded the numbers of students to get classes of 20 students and calculated the number of adults working in the school by scaling the numbers given in Appendix Table 2 to the numbers of students in each high school.

Figure 3 panels A, B in the main text show the catchment area of each of the 11 high schools along with the relative community incidence in each of those schools, as well as the basic reproductive number (R_0) assigned to each of those schools for the part of the analysis where R_0 varies across campuses. The methodology used to determine the community incidence of each school catchment area is detailed in the next section.

To analyze the impact of schools having different transmission rates we assigned each school an R_0 value, but those values are rough approximations based on limited data and do not necessarily represent what actually happened in the schools during the academic year 2020–2021.

To assign R_0 to each school, we used the reported COVID-19 cases in each AISD school from the district's public dashboard on March 8, 2021 (*20*), as well as the total enrollment and staff data per school used by TEA for allocation of tests in the context of the K–12 COVID-19 testing project (*21*).

We then regressed the number of reported cases y on the total school population x and obtained a best fit line of the form: $y = y_0 + \alpha \cdot x = 5.82 + 0.0095 \cdot x$ with $R^2 = 0.44$, as shown in Appendix Figure 4.

We then assigned an R_0 in each school proportional to the square root of the ratio of reported cases y_i to predicted cases:

$$\hat{y}_i = y_0 + \alpha \cdot x_i$$

with a base value of $R_0 = 1$. For a school that reported y_i cases with a total population x_i we assigned the following:

$$R_{0,i} = \sqrt{\frac{y_i}{y_0 + \alpha \cdot x_i}}.$$

The values assigned to each school are listed in Appendix Table 3.

3.1. COVID-19 Incidence in School Catchment Areas

To calculate the relative community incidence of COVID-19 cases for each school we combine catchment area information from AISD and COVID-19 burden data in the Austin metropolitan statistical area (MSA).

We first obtain the cumulative COVID-19 hospitalization rate, h_j, per 100,000 persons for each postal code *j* in the Austin MSA from March 2020–January 11, 2021 (*22*); then, we calculate the average hospitalization rate in the metropolitan area, h_{MSA}. From there we computed the relative burden experienced by each postal code *j* as follows:

$$r_j = \frac{h_j}{h_{MSA}}.$$

Next, we estimated the proportion of students in each school *i* coming from postal code *j* (p_{ij}) by using the proportion of school *i*'s catchment area located in postal code *j* as a proxy. To do so, we use GIS data from AISD and Austin MSA (*23*,*24*).

We denote by A_i the area of the catchment area of school *i*, the area covered by postal (i.e., ZIP) code *j* (Z_j), and $A_i \cap Z_j$ the area of the intersection of the two. We then have,

$$p_{ij} = \frac{A_i \bigcap Z_j}{A_i}$$

Combining the two quantities we then estimate the relative community incidence s_i of each school as the weighted average of the postal codes relative burden via the following:

$$s_i = \sum_j p_{ij} r_j.$$

3.2. Additional Results

Appendix Table 4 gives the cumulative on-campus attack rate in each school for three allocation strategies: no testing, prorated allocation of 14-day total testing capacity, and optimal allocation of 14-day prorated total testing capacity. The results are given for the scenarios in

which all schools have different transmission rates (first three substantive columns), and when they all have the same transmission rate (R_0 of 1.0, last three columns). The prorated and optimal allocations when schools have different transmission rates correspond to the results shown in Figure 4 panels A, B.

The additional results below analyzing the 11 high schools in AISD assume rapid tests with a sensitivity of 95% for symptomatic individuals, 80% for asymptomatic people, and a 99% specificity, based on reported estimates of the Abbott BinaxNOW antigen tests (*10*,*11*).

Appendix Figure 5 shows results similar to those shown in Figure 4 panels A, B in the main text, but here the transmission rate in all schools is identical and equal to 1.0. The blue bars showing the optimal allocation in the left panel correspond to the diamonds shown in Figure 4, panel A (main text). Appendix Figure 6 shows results similar to those shown in Figure 5 (main text), except that here the schools have the same transmission risk of $R_0 = 1.0$.

Appendix Figure 7 shows the risk level of each school under an optimal allocation when the on-campus transmission rate used as input to the optimization problem is different from the actual transmission rate of each school. Specifically, we derived an optimal allocation assuming all schools have the same on-campus transmission rate R_0 of 1.0 when schools actually have different on-campus transmission rates. The gray dots correspond to the resulting risk levels under that allocation, while the blue dots correspond to the risk level achieved when using the correct transmission rate to derive the optimal allocation, and the orange dots correspond to a pro rata allocation. The risk of most schools ends up being similar under the two optimal allocations, with the allocation derived using the wrong transmission rates typically resulting with in a risk level that is closer to the optimized risk level than that of the pro rata allocation, with the exception of schools H and I for which the pro rata allocation happens to be very close to optimal in that scenario.

4. Toy System Results

Appendix Table 5 below contains the details of the numbers shown in Figure 1, panel A in the main text. It gives the expected proportion of students infected on-campus for different quarantine strategies, testing frequencies, and in-school R_0. Appendix Table 6 contains the

details of the numbers shown in Figure 2, panel A in the main text. It gives the proportion of school days students either miss school, infected or not, or are at school while infected.

5. Toy System Optimization

We show the results of the optimal test allocation on a toy system of hypothetical schools (Appendix Figures 8, 9, 14). There are six schools of 500 students each in this system, three with a low daily community incidence of new cases (35 per 100,000) and three with a high daily community incidence (70 per 100,000). In each of the two groups the schools have different in-school transmission rates, low (unmitigated $R_0 = 1.0$), moderate (unmitigated $R_0 = 1.5$), and high (unmitigated $R_0 = 2.0$).

Appendix Figure 8 shows the number of averted infections through surveillance testing with a 2-week testing frequency budget, compared to no surveillance testing, for both a prorated allocation and an optimal allocation. Using the distributions of on-campus infections for a school under the scenario without testing, and under a scenario with testing, we can calculate the number of averted infections through testing using inversion sampling. We denote by $F_{no\ testing}$ and $F_{testing}$ the cumulative distribution functions (CDF) for the number of on-campus infections of the scenarios without testing and with testing, respectively. We then generate 300 random numbers $U_j, j \in [1, 300]$, uniformly distributed between 0 and 1, and we calculate the number of averted infections as follows:

$$A_j = F^{-1}_{no\,testing}(U_j) - F^{-1}_{testing}(U_j), j \in [1, 300].$$

As we move from no testing to a prorated allocation, we decrease the risk of all schools, and when we move from the prorated allocation to an optimal allocation, the performance of the three lowest-risk schools worsens slightly, i.e., the low-low, low-moderate, and high-low schools (incidence-transmission pairs). Meanwhile the number of cases averted at the remaining three schools grows significantly; hence, the total system risk decreases in an optimal allocation.

Appendix Figure 9 shows the optimal allocation of tests to all schools under different testing budgets, with the 14 days column corresponding to the allocation that yields the distributions of averted cases shown in Appendix Figure 8. No matter the testing frequency, under an optimal allocation the testing capacity is diverted from the same three low-risk schools

to the higher-risk schools. The low-low school receives the fewest tests under all budgets, while the high-high school receives the most. For instance, for a budget that would allow us to test all students in the system every 10 days on average, it would be optimal to test all students in the high-high school every week, while it would only be necessary to test students in the low-low school every 4 weeks to achieve the same overall level of risk. As a result, the risk profiles of all schools are very similar under the optimal allocation below that shows the distribution of on-campus infections for all schools under prorated and optimal allocations (Appendix Figure 14).

6. Sensitivity Analysis

6.1. Quarantine Strategy and Imperfect Surveillance Tests

It is now widely accepted that antigen tests for COVID-19 are effective at detecting infectious people, but there have been debates regarding their true performance (*25*). As such, we ran some sensitivity analyses using imperfect surveillance tests. Specifically, we used a test sensitivity of 95% for symptomatic individuals, 80% for asymptomatic (including pre-symptomatic) people, and we used a specificity of 99%, corresponding to published estimates of the Abbott BinaxNOW tests (*10*,*11*). Appendix Figure 10 shows results similar to those shown in Figure 1A and 1B (main text), the proportion of students infected in schools under different testing frequencies, for the same two quarantine strategies considered in Figure 1 (main text), as well as a scenario using imperfect tests and classroom quarantines.

6.2. School Days Missed

In Figure 2, panel A (main text) we detail the proportion of school days missed for a school with low community incidence and moderate transmission risk, for two quarantine strategies. In Appendix Figure 11, we show analogous results for the other hypothetical schools considered in our system, as well as the case in which imperfect tests are used.

The results are qualitatively similar across schools. We notice that holding other factors constant, a higher community incidence leads to more school days missed as more introductions of the disease in the school lead to more students being quarantined.

The bottom panels in each figure consider the case in which entire classrooms are quarantined while using imperfect tests with 99% specificity and with 80% and 95% sensitivity for asymptomatic and symptomatic individuals, respectively. While these tests reduce cases to a

similar extent as perfect tests (see Appendix Figure 10) the false positives (students testing positive despite not being infected) lead to students missing more school time while healthy, with school days missed increasing with the testing frequency.

We can also see that when the transmission risk is high, increasing the testing frequency does not lead to more school days missed when quarantining entire classrooms. Indeed, when the transmission risk is low enough some of the infected individuals found through surveillance testing would not infect anyone else, but entire classrooms are still quarantined, so that more frequent testing leads to more missed days. On the other hand, when the transmission rate is high more frequent testing allows us to find infected individuals earlier, before more infections occur, thus breaking transmission chains. This effect is also seen by looking at the proportion of days in school while infected when only households are quarantined: when the transmission risk is low that proportion decreases slowly as testing increases while it decreases dramatically as testing frequency increases when transmission risk is high.

6.3. Quarantine Duration and Contacts Quarantined

While many school districts have used a policy of quarantining contacts of a person testing positive for COVID-19 for 14 days, the Centers for Disease Control and Prevention (CDC) has continually been updating its interim guidance throughout the pandemic, saying in February 2021, that 10 days of isolation were sufficient in most cases, and in January 2022, it further shortened the isolation period to 5 days (*26*). We evaluated the impact of shorter isolation periods, either 7 days or 10 days, and compared it with our baseline assumption of a 14-day isolation period. Appendix Figure 12 shows the tradeoff between reducing infections and minimizing missed school days for different quarantine strategies at various testing frequencies for schools with a moderate transmission risk.

The different quarantine strategies are represented by different marker types and darker colors indicate more frequent surveillance testing. While quarantining entire classrooms for longer periods reduces infections more than shorter quarantines, it also leads to more school days missed for students. When testing is frequent enough, nearing weekly testing, longer quarantines are only marginally more effective at preventing infections (points closer to the x-axis) at the expense of more school days missed (points further from the y-axis).

6.4. Total Testing Budget

One way to visualize the allocation of tests across a set of schools is to graph the risk level of all schools as a function of the testing frequency in the same graph. Appendix Figure 13 shows the risk level of each of the six hypothetical schools in the system we consider, as we move from no surveillance testing to weekly testing. The risk of each school is again defined as the average of the expected on-campus infection rate and CVaR.

As the testing frequency increases the risk of each school decreases. The objective of our optimization is to find the lowest horizontal line on the graph such that the testing budget is respected. A horizontal line corresponds to all schools having the same risk, unless some school has reached the maximum testing frequency of 7 days, or a school does not need any testing to reach the same risk level as the other schools.

The left y-axis represents each school's risk, while the right y-axis represents the necessary budget required to achieve the corresponding maximum risk across schools. We can see that the lower the risk across schools becomes, the more expensive it becomes to further decrease it; to achieve a similar decrease requires much more frequent testing, so many more tests every week.

Given a certain budget we can draw a horizontal line at the corresponding point on the right axis and the intersection of this line with each of the schools' curves gives us the optimal allocation that minimizes the maximum risk across schools.

We can then verify that the full risk profiles of the six schools are very similar under the optimal allocation for the two budgets shown by the horizontal lines above. Appendix Figure 14 shows the distribution of on-campus infections in all the schools for three testing strategies. The no testing strategy shows the risk of each school without testing, the pro rata allocation shows the risk of all schools under the suboptimal allocation in which all schools receive the same number of tests, while under the optimal allocation all schools have a similar risk profile, and the total system risk is lowest.

6.5. Objective Function Optimized

In Appendix Figure 15 we show the sensitivity of the optimal allocation of tests in each school as we parametrically vary the objective function. We consider two testing budgets, first a budget in which all students can be tested every 4 weeks on average, and then every 2 weeks.

In the left panels we fix the weight of the CVaR term to 50%, and thus we have equal weight for the expected value of the infection rate when defining the risk of each school, $R(s)$, and we vary the CVaR level β. That is we solve the problem ($P_{50\%\beta}$) where β goes from 5% to 95%. In the middle panel we fix $\beta = 90\%$ and we solve ($P_{w,90\%}$) for w increasing from 0% to 100%, i.e., increasing the weight on the CVaR term. In the right panels we solve the problem (P_{total}), which aims to minimize the total system-wide expected infections.

When we only have a budget to test students every 4 weeks the impact of w and β on the solution of ($P_{w\beta}$) is limited, with only the school with the pair of low community incidence and moderate R_0 being allocated marginally more tests as w and β increase.

However, when we have a budget to test students every 2 weeks, we see much more variation in the allocation. This comes from the fact that with that budget the school with the pair of high community incidence and high R_0 is being allocated nearly enough tests to test weekly. As can be seen in the earlier Appendix Figure 13, the risk of that school does not change much as testing changes from every 9 days to every 7 days, so that small changes in w or β can impact the school risk enough to then cause large changes in the allocations to the other schools. While the changes in allocation for the school with high community incidence and high R_0 can seem large for small changes in the school risk parameters, the allocations to the other schools do not change drastically.

Lastly, in the right panels we see that when minimizing the total infections across all schools the same schools receive more tests than under a pro rata allocation, but there tends to be smaller differences in the number of tests allocated across schools as all schools receive a share closer to their pro rata allocation.

References

1. Bilinski A, Salomon JA, Giardina J, Ciaranello A, Fitzpatrick MC. Passing the Test: A Model-Based Analysis of Safe School-Reopening Strategies. [Internet]. Ann Intern Med. 2021;174:1090–100. PubMed https://doi.org/10.7326/M21-0600

2. US Census Bureau. Living arrangements of children under age 18 [cited 2021 Apr 14]. https://www.census.gov/library/visualizations/2016/comm/cb16-192_living_arrangements.html

3. Madewell ZJ, Yang Y, Longini IM Jr, Halloran ME, Dean NE. Household transmission of SARS-CoV-2: a systematic review and meta-analysis. JAMA Netw Open. 2020;3:e2031756. PubMed https://doi.org/10.1001/jamanetworkopen.2020.31756

4. Dur U, Morrill T, Phan W. Family ties: school assignment with siblings [cited 12 Sep 2022]. https://thayermorrill.wordpress.ncsu.edu/files/2019/06/FamilyTies.pdf

5. He X, Lau EHY, Wu P, Deng X, Wang J, Hao X, et al. Temporal dynamics in viral shedding and transmissibility of COVID-19. Nat Med. 2020;26:672–5. PubMed https://doi.org/10.1038/s41591-020-0869-5

6. He D, Zhao S, Lin Q, Zhuang Z, Cao P, Wang MH, et al. The relative transmissibility of asymptomatic COVID-19 infections among close contacts. Int J Infect Dis. 2020;94:145–7. PubMed https://doi.org/10.1016/j.ijid.2020.04.034

7. Gudbjartsson DF, Helgason A, Jonsson H, Magnusson OT, Melsted P, Norddahl GL, et al. Spread of SARS-CoV-2 in the Icelandic Population. N Engl J Med. 2020;382:2302–15. PubMed https://doi.org/10.1056/NEJMoa2006100

8. Davies NG, Klepac P, Liu Y, Prem K, Jit M, Eggo RM; CMMID COVID-19 working group. Age-dependent effects in the transmission and control of COVID-19 epidemics. Nat Med. 2020;26:1205–11. PubMed https://doi.org/10.1038/s41591-020-0962-9

9. Austin Independent School District. Health FAQs [cited 2021 Apr 14]. https://www.austinisd.org/openforlearning/healthsafety/health-faqs

10. US Food and Drug Administration. Abbott BinaxNOW COVID-19 Ag CARD instructions for use and characteristics [cited 2021 Apr 19]. https://www.fda.gov/media/141570/download

11. Pollock NR, Jacobs JR, Tran K, Cranston AE, Smith S, O'Kane CY, et al. Performance and implementation evaluation of the Abbott BinaxNOW Rapid Antigen Test in a high-throughput drive-through community testing site in Massachusetts. J Clin Microbiol. 2021;59:e00083-21. PubMed https://doi.org/10.1128/JCM.00083-21

12. Zhang J, Litvinova M, Wang W, Wang Y, Deng X, Chen X, et al. Evolving epidemiology and transmission dynamics of coronavirus disease 2019 outside Hubei province, China: a descriptive and modelling study. Lancet Infect Dis. 2020;20:793–802. PubMed https://doi.org/10.1016/S1473-3099(20)30230-9

13. Acerbi C, Tasche D. Expected shortfall: a natural coherent alternative to value at risk. Econ Notes. 2002;31:379–88. https://doi.org/10.1111/1468-0300.00091

14. Rockafellar RT, Uryasev S. Optimization of conditional value-at-risk. Journal of Risk. 2000;2:21–41. https://www.ise.ufl.edu/uryasev/files/2011/11/CVaR1_JOR.pdf

15. Powell MJD. On trust region methods for unconstrained minimization without derivatives. Math Program. 2003;97:605–23. https://doi.org/10.1007/s10107-003-0430-6

16. Virtanen P, Gommers R, Oliphant TE, Haberland M, Reddy T, Cournapeau D, et al.; SciPy 1.0 Contributors. SciPy 1.0: fundamental algorithms for scientific computing in Python. Nat Methods. 2020;17:261–72. PubMed https://doi.org/10.1038/s41592-019-0686-2

17. Austin Independent School District. About our schools, high schools [cited 2021 Jun 16]. https://www.austinisd.org/schools/level/H

18. Texas Education Agency. Student enrollment reports [cited 2021 Apr 14]. https://rptsvr1.tea.texas.gov/adhocrpt/adste.html

19. KVUE. Austin ISD reports 2 weeks of declining cases; 18% of student population back to in-person learning 2021 [cited 2021 Apr 14]. https://www.kvue.com/article/news/education/schools/austin-isd-reports-2-weeks-of-declining-cases/269-1d56a09b-0b89-44b6-b37b-dbe7ffc7d3c2

20. Austin Independent School District. COVID-19 dashboard [cited 2021 Jun 17]. https://www.austinisd.org/dashboard

21. Texas Education Agency. Texas K–12 COVID-19 testing project [cited 2021 Apr 13]. https://tea.texas.gov/texas-schools/health-safety-discipline/covid/covid-19-support-public-health-orders#project

22. University of Texas at Austin COVID-19 Modeling Consortium. Heterogeneous burden of the COVID-19 pandemic in central Texas [cited 2021 Apr 25]. https://sites.cns.utexas.edu/sites/default/files/cid/files/austin_covid-19_spatial_burden_report.pdf

23. Austin Independent School District. School maps/GIS [cited 2021 Nov 13]. https://www.austinisd.org/planning-asset-management/school-maps-gis

24. City of Austin. GIS data [cited 2021 Nov 13]. https://austintexas.gov/department/gis-data

25. Mina MJ, Peto TE, García-Fiñana M, Semple MG, Buchan IE. Clarifying the evidence on SARS-CoV-2 antigen rapid tests in public health responses to COVID-19. Lancet. 2021;397:1425–7. PubMed https://doi.org/10.1016/S0140-6736(21)00425-6

26. US Centers for Disease Control and Prevention. Interim guidance on duration of isolation and precautions for adults with COVID-19 [cited 2021 Apr 19]. https://www.cdc.gov/coronavirus/2019-ncov/hcp/duration-isolation.html

Appendix Table 1. School day schedule used in a model for COVID-19 test allocation strategy to mitigate SARS-CoV-2 infections across school districts*

Time	Context	Interactions
7:30–8:00 AM	Bus	19 students and 1 bus driver
8:00 AM–12:00 PM	Classroom	19 students and 1 teacher
12:00–1:00 PM	Break	9 students and 2 adults
1:00–3:00 PM	Classroom	19 students and 1 teacher
3:00–3:30 PM.	Bus	19 students and 1 bus driver

*The interactions column indicates the number of contacts a single student has in each context. The individuals that a student interacts with are set at the beginning of a simulation and stay the same throughout.

Appendix Table 2. Transmission parameters used in a model for COVID-19 test allocation strategy to mitigate SARS-CoV-2 infections across school districts

Parameter	Value	Source
Simulation duration	10 weeks	
No. students	500	
No. adults in school	25 teachers, 25 bus drivers, 16 staff	
τ: proportion symptomatic	20% of children, 57% of adults	Davies et al., Gudbjartsson et al. (*7*,*8*)
w_A: relative infectiousness of asymptomatic persons	2/3	He et al. (*6*)
d_{inc}: duration of incubation period	$d_{inc} \approx$ *Triangular*(3.2, 5.2, 7.2) (in days)	Zhang et al. (*12*)
d_{pre}: duration of pre-(a)symptomatic period	$d_{pre} \approx d_{inc}$ * *Triangular*(0.458, 0.558, 0.658) (average 2.9 d)	He et al. (*5*)
d_S: duration of (a)symptomatic period	$d_{inc} \approx$ *Triangular*(4, 8, 12) (in days)	He et al. (*5*)
Household attack rate	16.6%	Madewell et al. (*3*)
R_0: unmitigated basic reproduction number of children	1.0, 1.5, 2.0	
β: probability of infection in a half-hour for individual with infectiousness of 1.0	Fitted to R_0	
Daily community incidence	35 or 70 per 100,000	Average high and low incidence estimated over several weeks in Austin, TX during winter 2020–2021

Appendix Table 3. List of high schools from Austin Independent School District included in a model for COVID-19 test allocation strategy to mitigate SARS-CoV-2 infections across school districts*

School code	School name	No. students	Relative incidence†	School R_0
A	LBJ	60	1.95	1.41
B	Navarro	100	1.5	0.8
C	Northeast Early College	80	1.5	0.94
D	Eastside Memorial	40	1.49	0.87
E	Travis	80	1.18	0.84
F	Crockett	100	1.04	0.95
G	Akins	180	1.0	0.88
H	Anderson	140	0.7	1.1
I	Austin	140	0.58	1.26
J	McCallum	120	0.54	0.79
K	Bowie	180	0.37	0.98

*Includes assigned parameter values.
†Relative community incidence values are calculated by weighing the relative total attack rates of COVID-19 of the ZIP codes calculated in (*23*) using the proportion of students coming from each ZIP code as a weight. Schools are ordered according to their relative incidence.

Appendix Table 4. Median proportion of students infected in a model for COVID-19 test allocation strategy to mitigate SARS-CoV-2 infections across school districts*

School	Different transmission rates†			Same transmission rate‡		
code	No testing	Prorated allocation	Optimal allocation	No testing	Prorated allocation	Optimal allocation
A	14 (0.9–45.6)	4.0 (0.1–22.9)	2.2 (0–15)	7.3 (0.4–34.2)	2.7 (0.1–17)	1.6 (0–10.8)
B	5.3 (0.4–16.4)	1.9 (0.1–9.6)	1.4 (0–8.4)	7.2 (0.6–25.5)	2.6 (0.1–13.6)	1.5 (0–8.8)
C	6.3 (0.4–23.7)	2.1 (0.1–11.9)	1.3 (0–8.9)	6.4 (0.4–23.5)	2.4 (0.1–14)	1.5 (0–10.2)
D	3.6 (0–31.3)	1.8 (0–13.7)	1.0 (0–8.7)	4.3 (0–33.7)	2.1 (0–16.7)	1.1 (0–9.5)
E	3.9 (0.1–21.3)	1.5 (0–9.5)	1.3 (0–8.3)	4.6 (0.1–26.4)	1.7 (0–11.7)	1.3 (0–9.5)
F	4.3 (0.2–22.1)	1.7 (0–10)	1.4 (0–8.7)	4.3 (0.1–23.6)	1.8 (0–11)	1.4 (0–9.3)
G	4.3 (0.6–13.7)	1.6 (0.1–7.7)	2.0 (0.1–7.6)	5.7 (0.6–17.4)	2.1 (0.1–7.1)	2.6 (0.2–8.8)
H	4.6 (0.2–23.6)	1.5 (0–9.1)	1.4 (0–8.8)	3.2 (0.1–19.1)	1.3 (0–7.6)	1.7 (0.1–9.3)
I	4.8 (0.1–26.8)	1.3 (0–8.6)	1.2 (0–8.4)	3.1 (0.1–17.9)	0.9 (0–6.4)	1.4 (0–9.4)
J	1.7 (0–11.4)	0.7 (0–6.3)	1.1 (0–8.8)	2.2 (0–16.3)	1.0 (0–7.3)	1.2 (0–9.8)
K	1.6 (0–13)	0.7 (0–5)	1.1 (0–8.6)	1.6 (0–12.1)	0.6 (0–5.2)	1.3 (0–9.7)
Total	5.8 (3.1–9.6)	2.3 (1.1–4.1)	2.1 (0.9–4)	5.7 (2.9–9.5)	2.3 (1.1–4)	2.3 (1–4.1)

*Values represent % (95%CI) of students infected on-campus across 300 simulations for each school. The prorated and optimal allocations both correspond to total testing capacity every 14 days.
†Cumulative on-campus attack rates when each school has a different transmission rate.
‡Cumulative on-campus attack rates when all schools have the same transmission rate (R_0 = 1.0).

Appendix Table 5. Expected proportion of students infected on-campus over 10 weeks under different scenarios in a model for COVID-19 test allocation strategy to mitigate SARS-CoV-2 infections across school districts*

		Cumulative incidence rate, % (95% CI)		
Quarantine strategy	Testing frequency, d	Low transmission	Moderate transmission	High transmission
Household + class†	None	4.0 (0.8–9.1)	9.3 (1.8–19.6)	18.2 (4.8–35.7)
	28	2.3 (0.6–5.1)	4.2 (0.7–9.2)	7.0 (2.1–14.6)
	21	2.0 (0.3–4.8)	3.7 (0.8–8.0)	5.5 (1.3–12.1)
	14	1.5 (0.2–3.3)	2.9 (0.6–6.2)	4.1 (1.0–8.3)
	7	1.0 (0.1–2.5)	1.5 (0.2–3.8)	2.1 (0.3–4.8)
Household only‡	None	6.1 (1.1–15.1)	19.4 (2.9–41.5)	50.0 (21.1–80.8)
	28	3.7 (0.6–9.2)	10.5 (1.9–24.5)	26.6 (1.6–52)
	21	3.3 (0.5–8.7)	8.8 (1.0–23.4)	22.3 (3.6–49.4)
	14	2.8 (0.4–7.0)	6.3 (0.8–15.6)	14.7 (1–35.2)
	7	1.2 (0.1–3.2)	2.1 (0.2–5.4)	3.4 (0.4–8)

*Each column represents a different in-school R_0. We show results for increasing testing frequencies, from no testing to weekly testing.
†Class and households quarantined when a person tests positive.
‡Only households quarantined when a person tests positive.

Appendix Table 6. Expected proportion of school days students miss or are in school while infected for a school with moderate transmission rate in a model for COVID-19 test allocation strategy to mitigate SARS-CoV-2 infections across school districts*

		Proportion of school days, % (95% CI)		
Quarantine strategy	Testing frequency, d	At school infected	Missed school not infected	Missed school infected
Household + class†	None	1.4 (0.3–2.8)	5.3 (1.3–10.5)	0.6 (0.1–1.3)
	28	0.6 (0.1–1.2)	6.5 (2.0–12.0)	0.6 (0.1–1.2)
	21	0.5 (0.2–1.0)	6.8 (2.6–11.9)	0.5 (0.2–1.0)
	14	0.4 (0.1–0.7)	7.3 (2.9–12.1)	0.5 (0.2–0.9)
	7	0.2 (0.1–0.3)	7.4 (3.4–12.0)	0.5 (0.2–0.8)
Household only‡	None	3.0 (0.5–6.5)	0.6 (0.2–0.9)	0.4 (0.1–0.7)
	28	1.6 (0.4–3.5)	0.7 (0.3–1.3)	0.6 (0.2–1.2)
	21	1.3 (0.3–2.8)	0.8 (0.3–1.4)	0.6 (0.2–1.2)
	14	0.8 (0.2–1.8)	0.8 (0.4–1.4)	0.6 (0.2–1.3)
	7	0.3 (0.1–0.5)	0.6 (0.3–1.0)	0.5 (0.2–1.0)

*Each column represents a different type of day. We show results for increasing testing frequencies, from no testing to weekly testing.
†Class and households quarantined when a person tests positive.
‡Only households quarantined when a person tests positive.

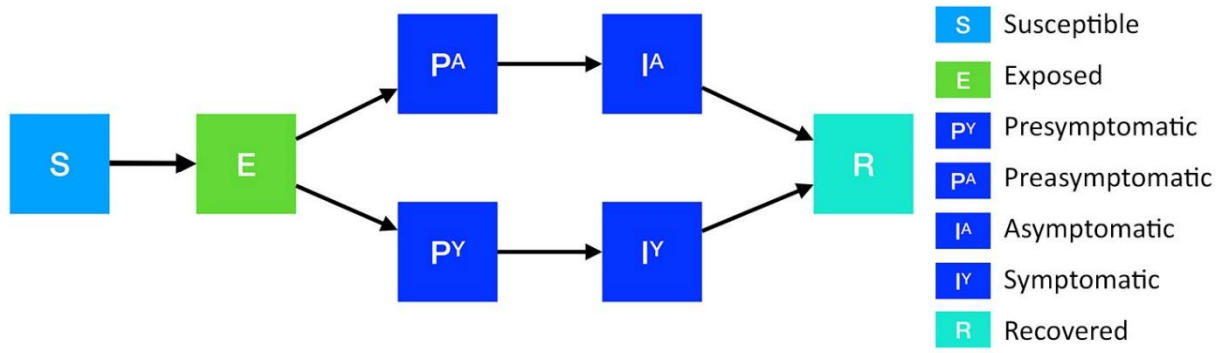

Appendix Figure 1. Schematic of the agent-based SEPIR model used for a COVID-19 test allocation strategy to mitigate SARS-CoV-2 infections across school districts. Upon infection, susceptible individuals (S) progress to exposed (E) and then to either pre-symptomatic infectious (PY) or pre-asymptomatic infectious (PA), from which they move to symptomatic infectious (IY) and asymptomatic infectious (IA), respectively. All cases eventually progress to a recovered class, where they remain protected from future infection (R). The proportion of individuals who become asymptomatic rather than symptomatic varies between children and adults. SEPIR, susceptible-exposed-presymptomatic-infectious-recovered.

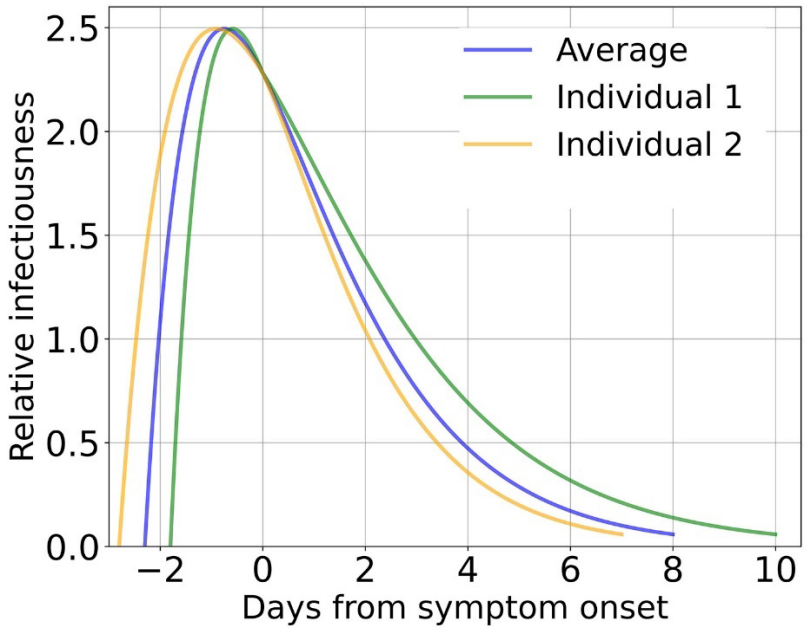

Appendix Figure 2. Relative infectiousness profile in a model for COVID-19 test allocation strategy to mitigate SARS-CoV-2 infections across school districts. The graph shows infectiousness through time of 3 infected persons relative to symptom onset. The average person (blue line) stays in the presymptomatic or preasymptomatic compartment for 2.3 days and the asymptomatic or symptomatic compartment for 8 days. Individual 1 spends 1.8 days the presymptomatic and 10 days in the infectious compartments. Individual 2 spends 2.8 in the presymptomatic and 7 days in the infectious compartments.

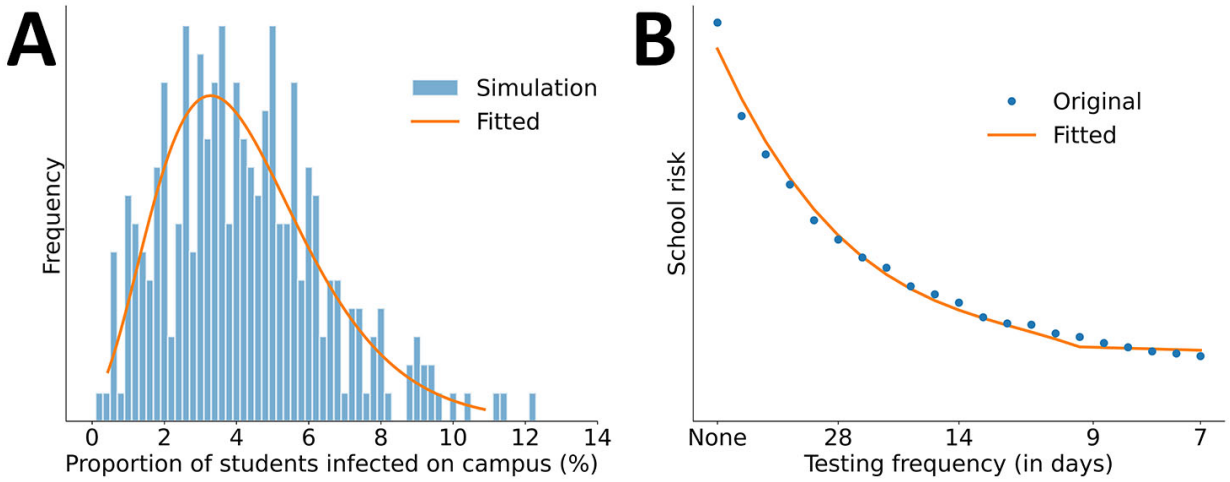

Appendix Figure 3. Processing results from the transmission model for COVID-19 test allocation strategy to mitigate SARS-CoV-2 infections across school districts. Processing results provide inputs to the optimization model. In both graphs the school used has an unmitigated R_0 of 1.5, daily community incidence of 35 cases per 100,000 population, and perfect COVID-19 tests are used. A) Shows frequency after fitting a gamma distribution to the results of the simulation model. The blue bars represent the number of students infected on a campus across 300 simulations. The orange line represents the best fitted nonnegative gamma distribution. Results correspond to a testing frequency of once every 4 weeks. B) School risk based on testing frequency. The graph shows fitting of a non-increasing curve to the risk of a school as a function of the proportion of students tested weekly. The blue dots represent the risk levels calculated by using the fitted gamma distributions. The orange line represents the best fitted curve used as input to the optimization model. The specific risk metric used is half the sum of the on-campus infection rate's expected value and 90% conditional value-at-risk.

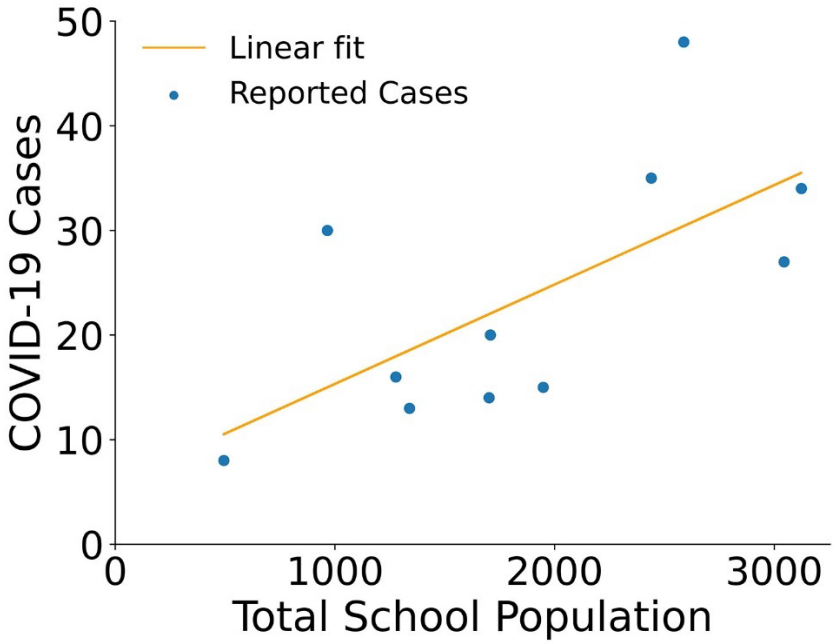

Appendix Figure 4. Reported COVID-19 cases in AISD high schools as a function of total school population used in a model for COVID-19 test allocation strategy to mitigate SARS-CoV-2 infections across school districts. COVID-19 cases were obtained from AISD's public dashboard (https://www.austinisd.org/dashboard) on March 8, 2021. School population includes total enrollment and staff. The orange line represents the best linear fit. AISD, Austin Independent School District

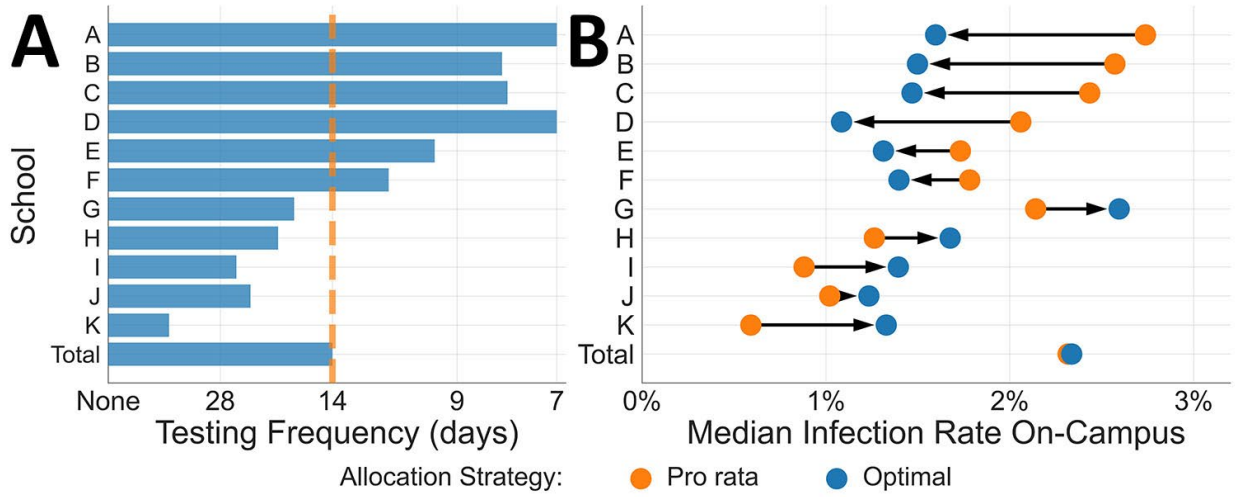

Appendix Figure 5. Testing frequency and median COVID-19 infection rate of 11 high schools in the Austin Independent School District used in a model for COVID-19 test allocation strategy to mitigate SARS-CoV-2 infections across school districts. A) Allocations for two testing strategies: pro rata, in which all schools test their students once per every 14 days (dashed orange line); optimized to minimize the maximum risk of any school, considering variation in community risk (blue bars). B) The median percent of students infected on-campus under the optimized strategy (blue) and pro rata strategy (orange), over a 10-week period. Arrows indicate increase or decrease in infection rate going from the pro rata to the optimal strategy. The model assumes all schools have the same transmission risk. Values are averages across 300 simulations. The model assumes that classrooms quarantine for 14 days after a positive test.

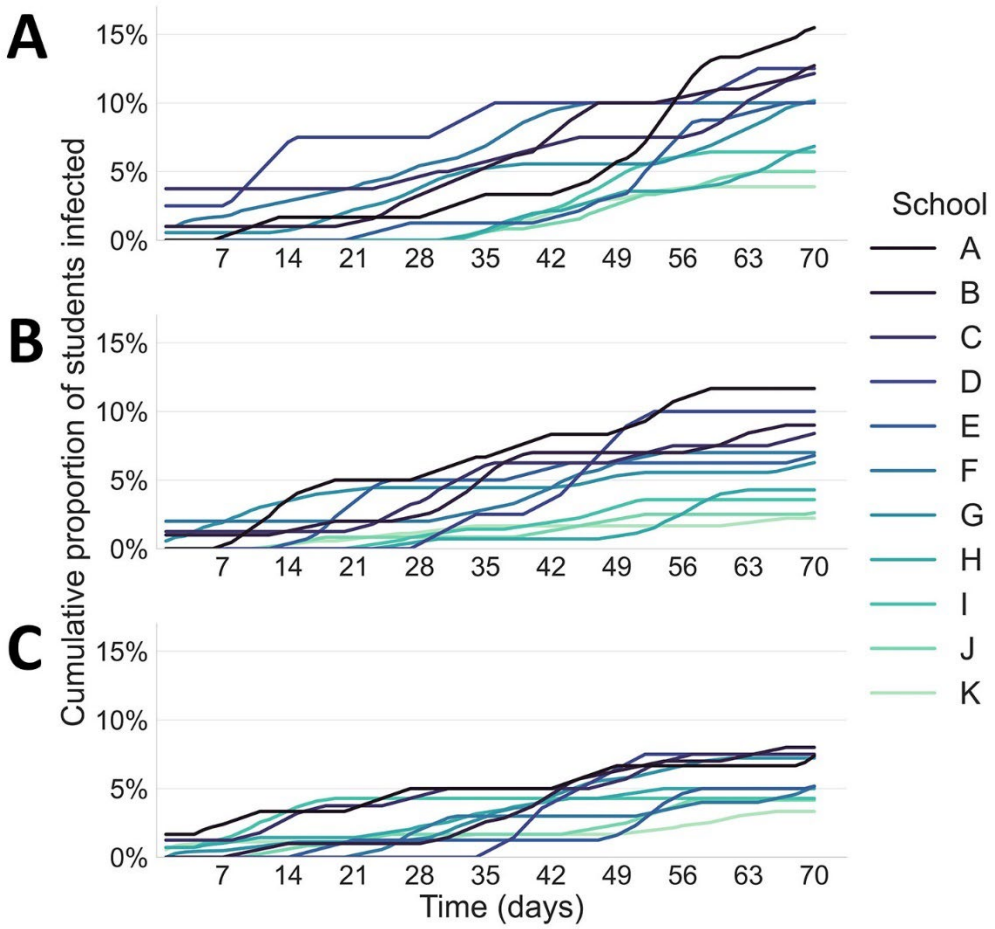

Appendix Figure 6. Cumulative proportion of students infected in a modeled COVID-19 test allocation strategy to mitigate SARS-CoV-2 infections across school districts. The graphs represent 3 testing scenarios: A) No testing; B) all schools test all students every 14 days; C) optimized allocation of tests based on schools having the same transmission risk, assuming a district-wide budget of one test per student every 14 days. Graphs show 11 high schools in the Austin Independent School District over a 10-week period. Schools are ordered from A–K based on community incidence in the school catchment area (from high to low). Graphs depict 7-day moving averages based on a single simulation for each scenario and school. To show representative projections, we selected the simulation that produced a cumulative attack rate closest to the median across all 300 simulations.

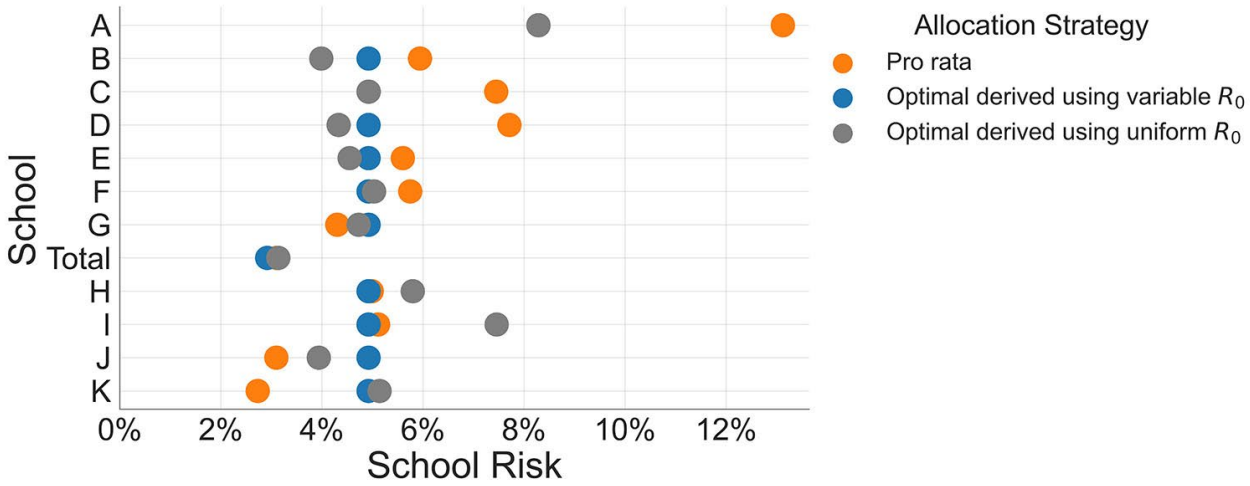

Appendix Figure 7. COVID-19 risk for schools used in a model for COVID-19 test allocation strategy to mitigate SARS-CoV-2 infections across school districts. We applied the model to 11 high schools in the Austin Independent School District. The graph shows the risk level of each school (A–K) under 3 possible testing allocations and a 14-day testing capacity when schools have different on-campus transmission rates. Risk was the objective value minimized in the optimization problem (*P*), defined as the average of the expected cumulative incidence (i.e., the mean across 300 simulations) and the projected tail risk. Blue dots correspond to the risk level under the optimal allocation obtained when we correctly assigned different on-campus transmission rates to each school. Gray dots correspond to the risk level obtained when the optimal allocation is obtained assuming all schools have the same on-campus reproduction number R_0 of 1.0. Orange dots correspond to the risk level under pro rata testing, in which all schools test their students once per every 14 days.

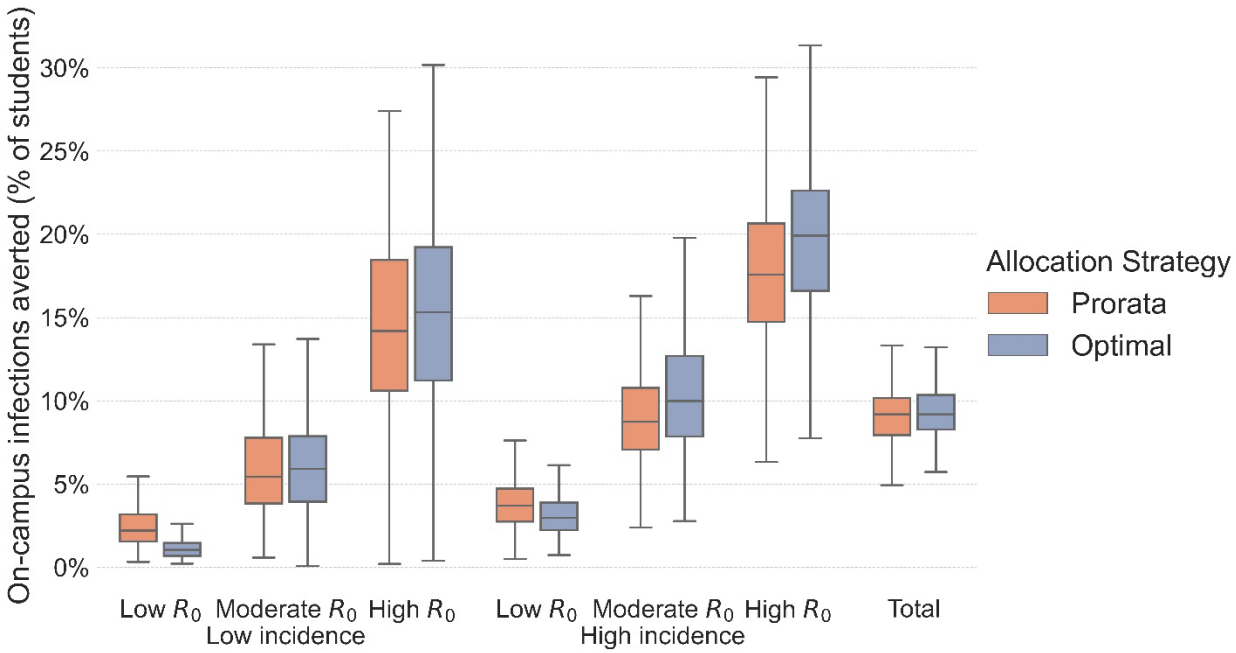

Appendix Figure 8. Proportion of on-campus infections averted in a model for COVID-19 test allocation strategy to mitigate SARS-CoV-2 infections across school districts. Averted on-campus infections are relative to no surveillance testing, for each of 6 different schools and the entire system over a 10-week period under 2 possible testing allocation strategies. In the modeled scenario, both allocation strategies have a budget to test students every 14 days. In the pro rata allocation, all schools test students every 14 days. When an individual tests positive, their entire classroom and household are quarantined for 14 days. In the optimal strategy, tests are allocated to minimize the maximum risk of any school, considering variation in community and in-school transmission risks. Boxes indicate interquartile range (IQR); horizontal bars inside boxes indicate median; whiskers indicate points that lie within 1.5 IQRs of the closest quartile.

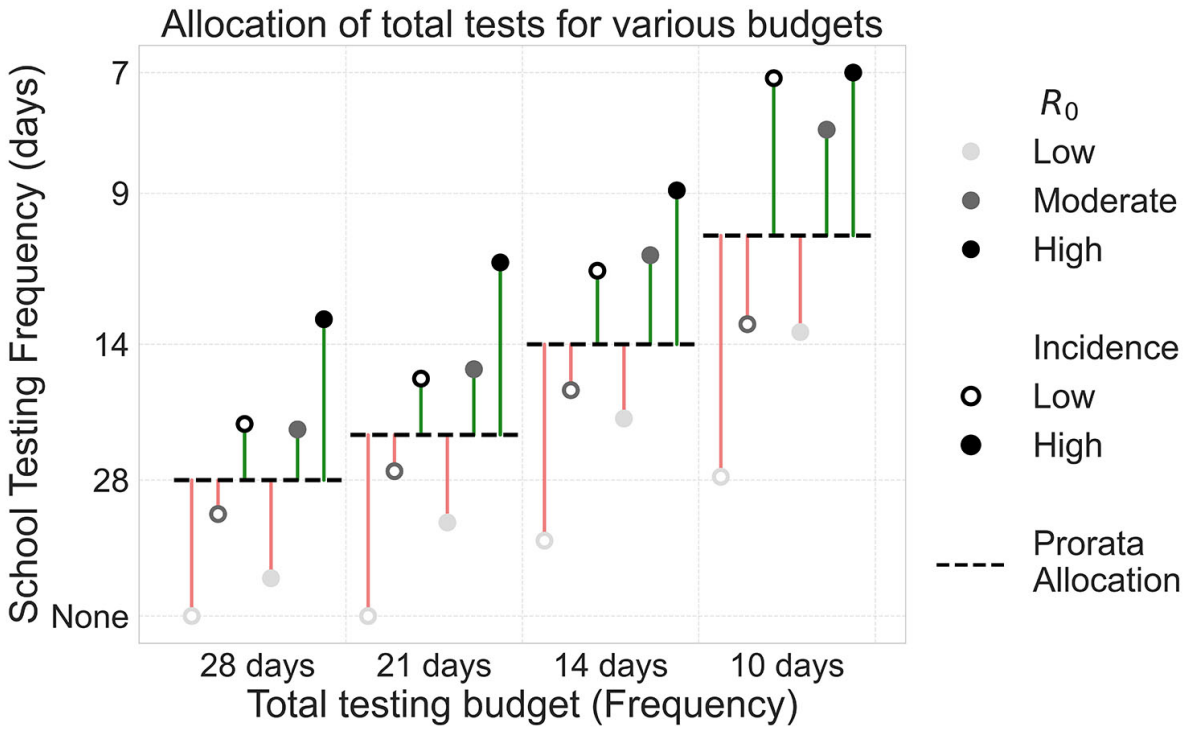

Appendix Figure 9. Optimal test allocations under different budgets in a model for COVID-19 test allocation strategy to mitigate SARS-CoV-2 infections across school districts. The horizontal dotted lines represent the prorated allocation for each budget. A green line indicates that a school receives more tests under our optimal allocation than under the prorated one, and a red line indicates a school receives fewer tests than the optimal allocation. Transmission risk has an R_0 value corresponding to 1.0 (low risk), 1.5 (moderate risk), 2.0 (high risk). Low community incidence is set at 35 new daily infections per 100,000 population; high community incidence is set at 70 new daily infections per 100,000 population. R_0, basic reproduction number.

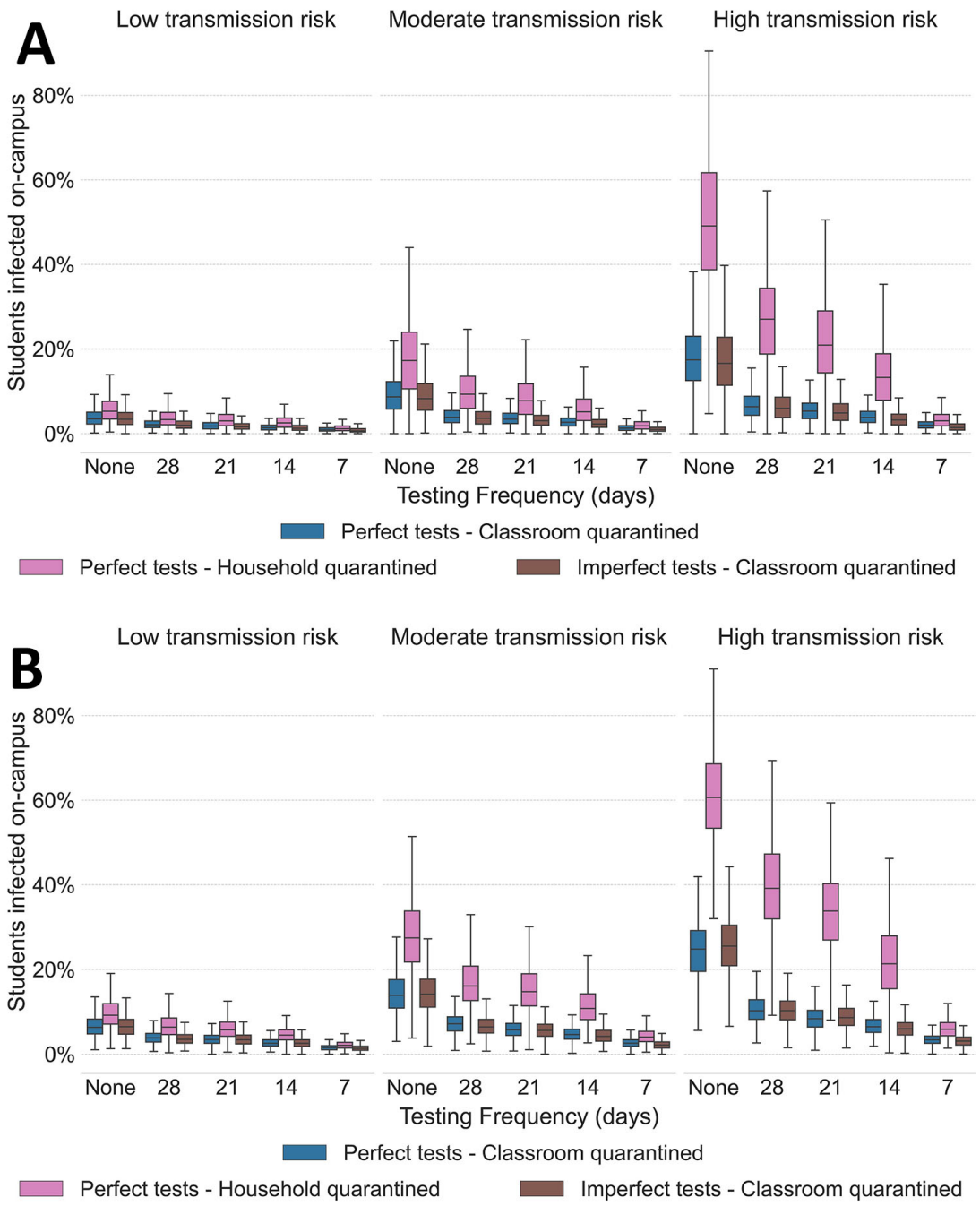

Appendix Figure 10. Projected effects of proactive SARS-CoV-2 testing in a model for COVID-19 test allocation strategy to mitigate SARS-CoV-2 infections across school districts. A) Low community incidence (35 new daily infections per 100,000 population). B) High community incidence (70 new daily infections per 100,000 population). We modeled fraction of students infected on campus depending on the frequency of proactive testing (none, or once per every 28, 21, 14, or 7 days) over a 10-week period in a school with 500 students. We modeled 3 scenarios (colors): entire classrooms are quarantined for 14 days after a positive test, by using either perfect or imperfect tests, or only households of persons testing

positive are quarantined for 14 days with perfect tests. Imperfect tests have a sensitivity of 95% for symptomatic individuals, 80% for asymptomatic (including pre-symptomatic) people, and we used a specificity of 99%, while perfect tests have 100% sensitivity and specificity. Transmission risk has an R_0 value corresponding to unmitigated basic reproduction numbers of 1.0 (low risk), 1.5 (moderate risk), 2.0 (high risk). The results are based on 300 stochastic simulations for each scenario. Boxes indicate interquartile range (IQR); horizontal bars inside boxes indicate median; whiskers indicate points that lie within 1.5 IQRs of the closest quartile. *R_0*, basic reproduction number.

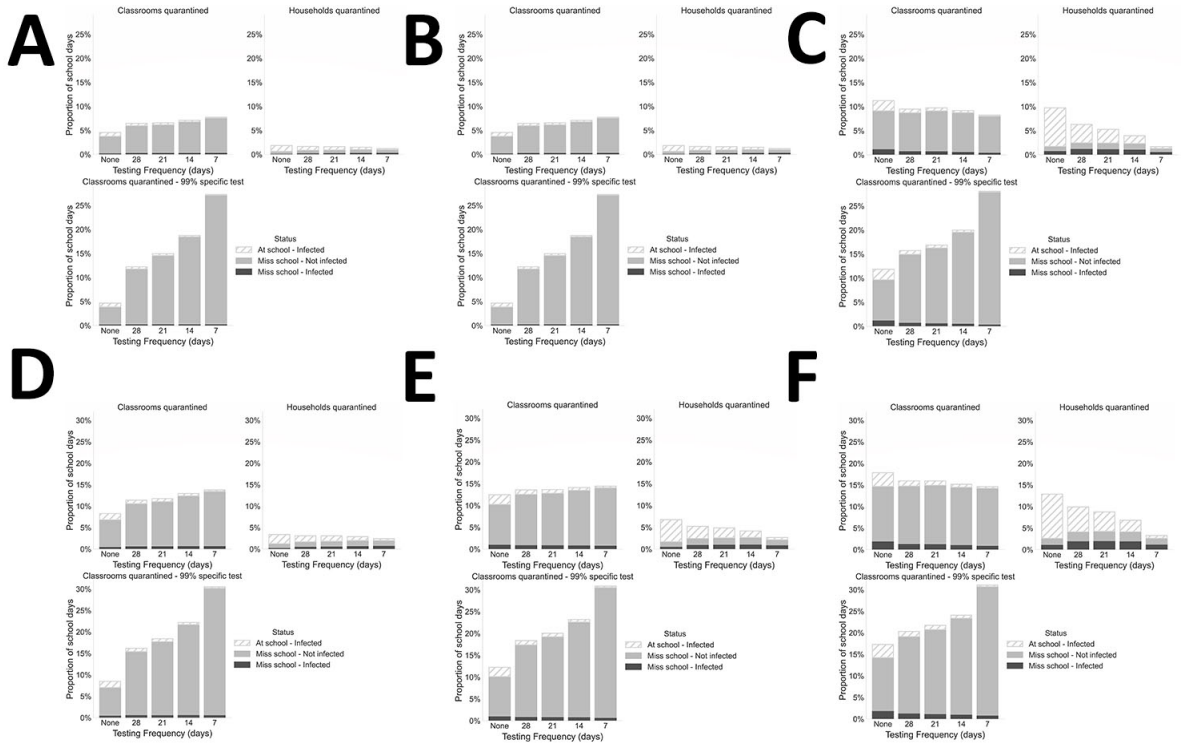

Appendix Figure 11. Effects of student testing on in-person attendance in a model for COVID-19 test allocation strategy to mitigate SARS-CoV-2 infections across school districts. A) Low community incidence (35 new daily infections per 100,000 population) and low transmission risk (R_0 = 1.0). B) Low community incidence and moderate transmission risk (R_0 = 1.5). C) Low community incidence and high transmission risk (R_0 = 2.0). D) High community incidence (70 new daily infections per 100,000 population) and low transmission risk (R_0 = 1.0). E) High community incidence and moderate transmission risk (R_0 = 1.5). F) High community incidence and high transmission risk (R_0 = 2.0). We modeled student attendance depending on the frequency of proactive testing (none, or once per every 28, 21, 14, or 7 days) over a 10-week period in schools with 500 students based on a total of 300 simulations for each scenario. Graphs show average number of school days missed due to isolation while infected, or while quarantined and disease-free, as well as average number of days in school while infected, depending on

the testing frequency. The top row of each figure corresponds to perfect tests where either entire classrooms or households only are quarantined after a positive test. The bottom rows correspond to tests with 99% specificity, 80% sensitivity for asymptomatic persons, and 95% sensitivity for symptomatic individuals, and entire classrooms quarantined after a positive test.

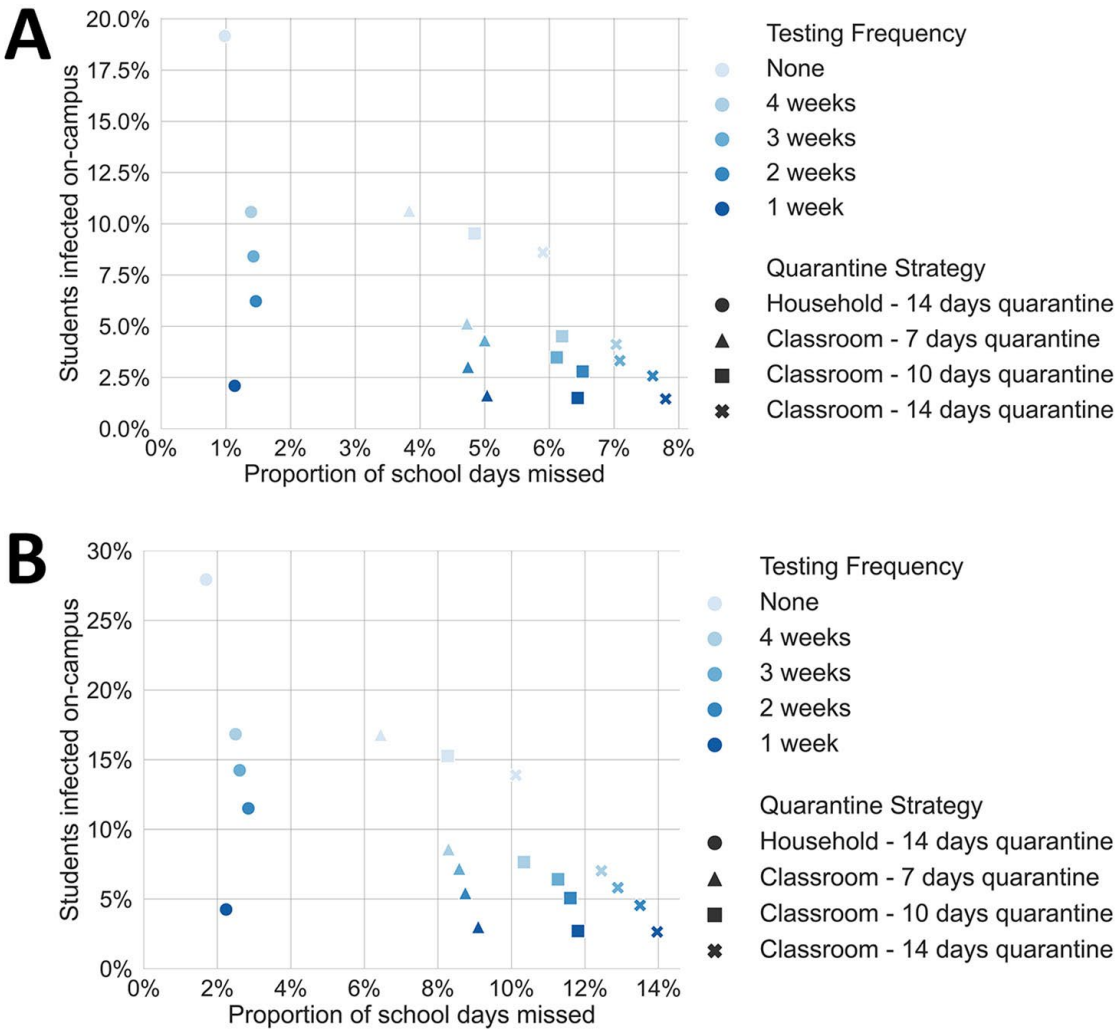

Appendix Figure 12. Tradeoff between infections prevented and school days missed for different quarantine strategies in a model for COVID-19 test allocation strategy to mitigate SARS-CoV-2 infections across school districts. A) Low community incidence (35 new daily infections per 100,000 population). B) High community incidence (70 new daily infections per 100,000 population). Each point represents the average proportion of students infected on-campus (vertical axis) and the average proportion of school days missed (horizontal axis) for 300 simulations over a 10-week horizon. Schools have an unmitigated R_0 of 1.5. R_0, basic reproductive number.

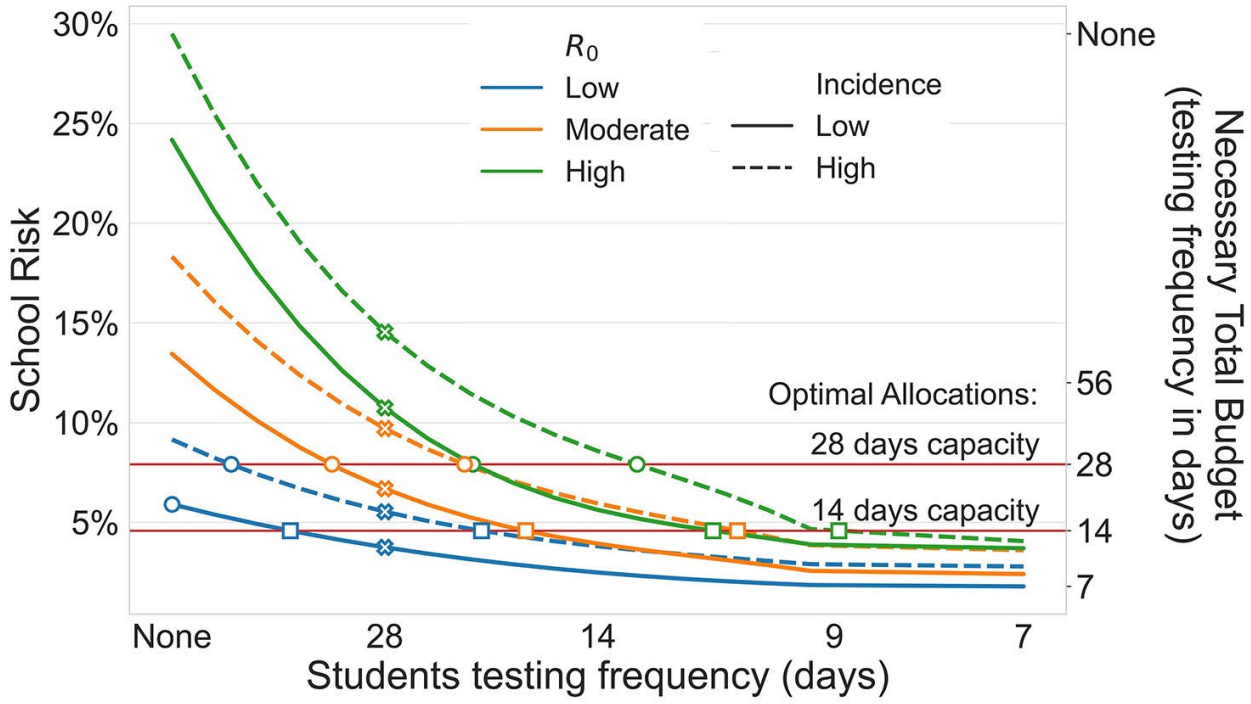

Appendix Figure 13. Individual school risks as testing frequency increases in a model for COVID-19 test allocation strategy to mitigate SARS-CoV-2 infections across school districts. The left axis indicates individual school risk for a given testing frequency. The right axis indicates the budget necessary to achieve a given risk level. The horizontal lines explicitly show the minimal risk attainable for system-wide testing capacities of 4 weeks and 2 weeks, with the circles and squares representing the schools' risk and testing level under the optimal allocations for these two budgets. The crosses represent the risk and allocation of each school under a prorated allocation of an every 4-weeks testing budget. Transmission risk has a value corresponding to unmitigated an R_0 of 1.0 (low risk), 1.5 (moderate risk), or 2.0 (high risk). Low community incidence corresponds to 35 new daily infections per 100,000 population and high community incidence corresponds to 70 new daily infections per 100,000 population. R_0, basic reproductive number.

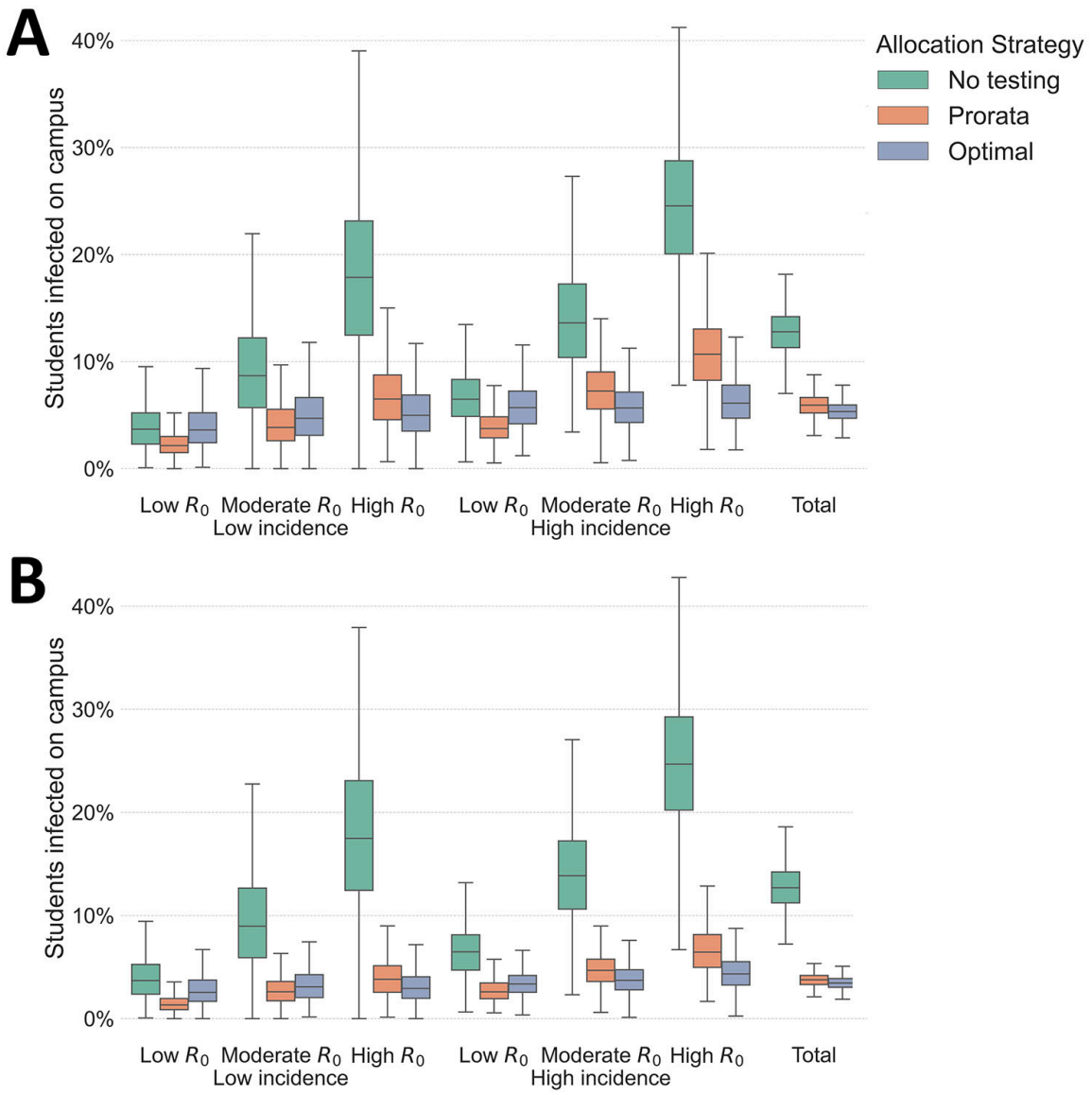

Appendix Figure 14. Distribution of the proportion of students infected on-campus in each school and in the entire school system in a model for COVID-19 test allocation strategy to mitigate SARS-CoV-2 infections across school districts. We modeled infections over a 10-week period under 3 possible testing strategies. The pro rata and optimal allocations use the same total testing budget for a testing frequency of every 4 weeks (A) or for a for a testing frequency of every 2 weeks (B). Boxes indicate interquartile range; horizontal bars inside boxes indicate median; whiskers indicate points that lie within 1.5 IQRs of the closest quartile. Transmission risk has a value corresponding to unmitigated an R_0 of 1.0 (low risk), 1.5 (moderate risk), or 2.0 (high risk). Low community incidence corresponds to 35 new daily infections per 100,000 population and high community incidence corresponds to 70 new daily infections per 100,000 population. R_0, basic reproductive number.

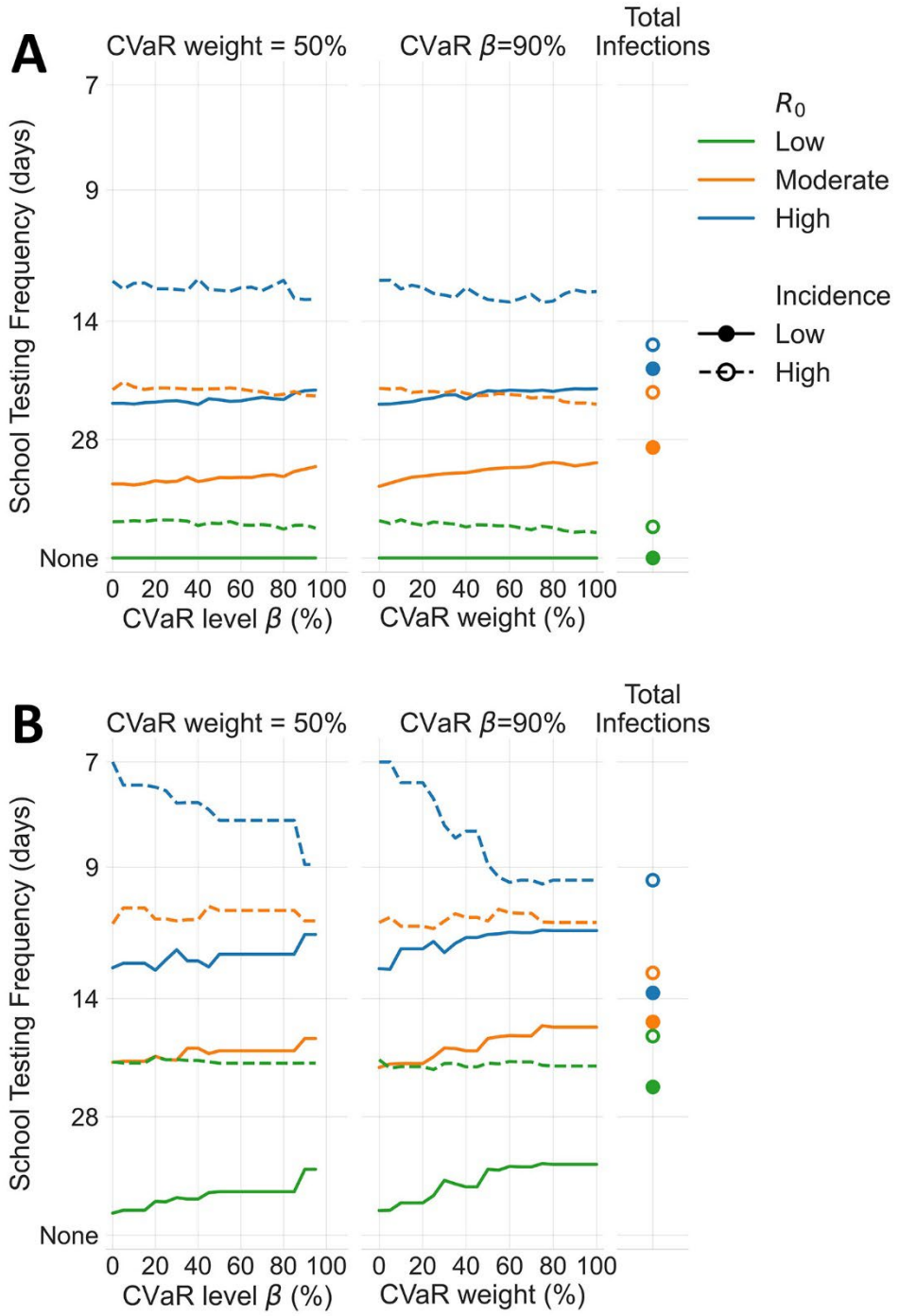

Appendix Figure 15. Optimal allocation to each school for different objective functions in a model for COVID-19 test allocation strategy to mitigate SARS-CoV-2 infections across school districts based on budgets for a testing frequency of 4 weeks (A), or for a testing frequency of 2 weeks (B). The left panels correspond to an objective function where the relevant quantile for CVaR increases from the 5% quantile to the 95% quantile, with the weight on the CVaR fixed at 50% (with the other 50% on the number of expected infections). The center panels correspond to an objective function where the weight of CVaR

term grows from 0% (expectation only) to 100% (CVaR only), with the CVaR level fixed at 90%. The right panels correspond to the optimal allocation obtained from minimizing the total number of on-campus infections across schools. Transmission risk has an R_0 value corresponding to unmitigated basic reproduction numbers of 1.0 (low risk), 1.5 (moderate risk), or 2.0 (high risk). CVaR, conditional value-at-risk; R_0, basic reproduction number.